THE DISPERSION RELATION OF ION CYCLOTRON WAVES

Marco Brambilla

IPP 4/209

November 1982

MAX-PLANCK-INSTITUT FÜR PLASMAPHYSIK

8046 GARCHING BEI MÜNCHEN

MAX-PLANCK-INSTITUT FÜR PLASMAPHYSIK

GARCHING BEI MÜNCHEN

THE DISPERSION RELATION OF ION CYCLOTRON WAVES

Marco Brambilla

IPP 4/209 November 1982

This report has been prepared under the contract JB1/9020
between the IPP-Euratom Association and JET.

Die nachstehende Arbeit wurde im Rahmen des Vertrages zwischen dem Max-Planck-Institut für Plasmaphysik und der Europäischen Atomgemeinschaft über die Zusammenarbeit auf dem Gebiete der Plasmaphysik durchgeführt.

IPP 4/209

THE DISPERSION RELATION OF ION CYCLOTRON WAVES

Marco Brambilla

November 1982

ABSTRACT - We review the dispersion relation of Ion Cyclotron waves in a plane-layered plasma model. A simple, yet accurate expansion valid for small ion Larmor radius (compared to the wavelength) and small electron inertia, is obtained, which is appropriate for use in the implementation of ray-tracing techniques. The propagation characteristics of waves in the vicinity of the ion cyclotron resonance and its first harmonic, as well as near the two-ion hybrid resonances in a multi-species plasma, are investigated in some detail.

This report has been prepared under the contract JB1/9020 between the IPP-Euratom Association and JET.

C O N T E N T

1. INTRODUCTION

Any detailed study of rf heating presupposes a thorough knowledge of the dispersion relation of the plasma in the relevant frequency range. In view of applications to ray-tracing and absorption studies for JET and ASDEX, we will review in this note the propagation characteristics of waves in the ion cyclotron frequency domain, in a simple plane-layered, one-dimensional geometry, which is a naive model of large tokamak plasmas. We will in particular devote some care to the derivation of the simplest yet accurate dispersion relation for these waves, and to the investigation of their behaviour in the critical regions, namely the vicinity of the cyclotron resonances and their first harmonic, and of the Two Ion Hybrid resonances.

The results presented are not new, but are scattered in the literature, and seem not always universally known. They are collected here as a convenient reference for further investigations in this field.

The standard model for such a study is a plasma slab, with magnetic field in the z-direction, and gradients in the x-direction (z replacing the toroidal and x the radial direction of a real tokamak). It is also assumed that the wave amplitudes are uniform in the y-direction (poloidal) so that their wavevector is

$$\vec{k} = k_\perp \hat{e}_x + k_{/\!/} \hat{e}_z \qquad (1)$$

$k_{/\!/}$ is constant (e.g. determined by the periodicity of the antenna), while $k_\perp$ is to be determined from the dispersion relation. Thus this model includes some, but not all, of the features of a tokamak plasma: the most important limitation being the exclusion of the rotational transform. It gives nevertheless valuable insight into the physics of ion cyclotron waves, unobscured by the complications of more realistic models.

The coordinate frame just introduced coincides with the local frame in which the plasma dielectric tensor is usually obtained /1/. Thus, introducing for convenience the dimensionless index $\vec{n} = \vec{kc}/\omega$, we write the dispersion relation in the form

$$(2) \qquad 0 = \begin{vmatrix} \varepsilon_{xx} - n_{//}^2 & \varepsilon_{xy} & \varepsilon_{xz} + n_\perp n_{//} \\ \varepsilon_{yx} & \varepsilon_{yy} - (n_\perp^2 + n_{//}^2) & \varepsilon_{yz} \\ \varepsilon_{zx} + n_\perp n_{//} & \varepsilon_{zy} & \varepsilon_{zz} - n_\perp^2 \end{vmatrix}$$

Using the symmetries

$$(3) \qquad \varepsilon_{xy} = -\varepsilon_{yx} \qquad \varepsilon_{xz} = \varepsilon_{zx} \qquad \varepsilon_{zy} = -\varepsilon_{yz}$$

we can rewrite Eq. (2) in the form

$$(4) \qquad 0 = \left(-n_\perp^2 + \varepsilon_{zz}\right)\left[\left(-n_\perp^2 - n_{//}^2 + \varepsilon_{yy}\right)\left(-n_{//}^2 + \varepsilon_{xx}\right) + \varepsilon_{xy}^2\right] + \varepsilon_{yz}^2\left(-n_{//}^2 + \varepsilon_{xx}\right) - \left(n_\perp n_{//} + \varepsilon_{xz}\right)^2\left(-n_\perp^2 - n_{//}^2 + \varepsilon_{yy}\right) + 2\varepsilon_{xy}\varepsilon_{yz}\left(n_\perp n_{//} + \varepsilon_{xz}\right)$$

The elements of the dielectric tensor are

(5)
$$\varepsilon_{xx} = 1 - \sum_j \frac{\omega_{pj}^2}{\omega^2} \sum_{n=-\infty}^{+\infty} \frac{n^2}{\lambda_j^2} I_n(\lambda_j) e^{-\lambda_j} \left(-x_{0j}\, Z(x_{nj})\right)$$

$$\varepsilon_{xy} = -\varepsilon_{yx} = i \sum_j \frac{\omega_{pj}^2}{\omega^2} \sum_{n=-\infty}^{+\infty} n \left[I_n(\lambda_j) - I_n'(\lambda_j)\right] e^{-\lambda_j} \left(-x_{0j}\, Z(x_{nj})\right)$$

$$\varepsilon_{yy} = 1 - \sum_j \frac{\omega_{pj}^2}{\omega^2} \sum_{n=-\infty}^{+\infty} \left\{ \frac{n^2}{\lambda_j} I_n(\lambda_j) + \right.$$

$$\left. + 2\lambda_j \left[I_n(\lambda_j) - I_n'(\lambda_j)\right] \right\} e^{-\lambda_j} \left(-x_{0j}\, Z(x_{nj})\right)$$

$$\varepsilon_{xz} = \varepsilon_{zx} = -\frac{n_\perp n_\parallel}{2} \sum_j \frac{\omega_{pj}^2}{\omega \Omega_{cj}} \frac{v_{thj}^2}{c^2} \sum_{n=-\infty}^{+\infty} \frac{n}{\lambda_j} I_n(\lambda_j) e^{-\lambda_j} x_{0j}^2 Z'(x_{nj})$$

$$\varepsilon_{yz} = -\varepsilon_{zy} = -i \frac{n_\perp n_\parallel}{2} \sum_j \frac{\omega_{pj}^2}{\omega \Omega_{cj}} \frac{v_{thj}^2}{c^2} \sum_{n=-\infty}^{+\infty} \left[I_n(\lambda_j) - I_n'(\lambda_j)\right] \cdot$$

$$\cdot\, e^{-\lambda_j}\, x_{0j}^2\, Z'(x_{nj})$$

$$\varepsilon_{zz} = 1 - \sum_j \frac{\omega_{pj}^2}{\omega^2} \sum_{n=-\infty}^{+\infty} I_n(\lambda_j) e^{-\lambda_j} \cdot x_{0j} x_{nj} Z'(x_{nj})$$

Here the first summation extends over the electrons and the various species of ions, and the following notations are used:

$$\lambda_j = \frac{1}{2}\frac{k_\perp^2 v_{thj}^2}{\Omega_{cj}^2} = \frac{1}{2} k_\perp^2 \rho_j^2 \qquad x_{nj} = \frac{\omega - n\Omega_{cj}}{k_\parallel v_{thj}} \tag{6}$$

The notations for the plasma and cyclotron frequencies of the electrons and ions are standard. Thermal velocities are defined as

$$v_{thj}^2 = \frac{2kT_j}{m_j} \tag{7}$$

$I_n(\lambda_j)$ denotes the n-th modified Bessel function, while Z (x) is the Plasma Dispersion Function /2/

$$Z(x) = \frac{1}{\sqrt{\pi}} \int_{-\infty}^{+\infty} \frac{e^{-u^2}}{u^2 - x}\, du + \sigma \sqrt{\pi}\, i e^{-x^2} \tag{8}$$

$$\sigma = 0 \quad \text{for } \operatorname{Im} x > 0$$
$$\sigma = 1 \quad \text{for } \operatorname{Im} x = 0$$
$$\sigma = 2 \quad \text{for } \operatorname{Im} x < 0$$

We are not interested in the solution of Eq. (2) as it stands, but rather in obtaining accurate approximations including all the relevant physics, and appropriate for applications to more complicated problems. This can be achieved by making use of the existence of two small parameters, namely the ratio between the ion Larmor radius and the perpendicular wavelength on the one hand, and the ratio between the masses of the electron and the ions on the other hand. In the following section we will develop Eq. (2) in these small parameters in turn, devoting some care to the identification of the significant contributions.

2. APPROXIMATE DISPERSION RELATION

a) Small Larmor Radius Development

It is convenient to develop first for small Larmor radii, without distinguishing between ions and electrons. Not all the elements of the dielectric tensor contribute significantly to the dispersion relation in this limit. For completeness however we will give here the first order development for all terms. We introduce the notations

$$
\begin{aligned}
\varepsilon_{xx} &= S - \sigma_1 n_\perp^2 \\
\varepsilon_{xy} &= -\varepsilon_{yx} = -i\left(D - \delta n_\perp^2\right) \\
\varepsilon_{yy} &= S - \sigma_2 n_\perp^2 \\
\varepsilon_{xz} &= \varepsilon_{zx} = -n_\perp n_{/\!/}\,\eta \\
\varepsilon_{yz} &= -\varepsilon_{zy} = -i n_\perp n_{/\!/}\,\xi \\
\varepsilon_{zz} &= P - \pi n_\perp^2
\end{aligned}
\tag{9}
$$

We define also the following dielectric tensor components expressed in 'rotating' coordinates (they are not needed in the study of the dispersion relation, but enter essentially in the determination of the wave polarisations and in the equations for power transport and absorption):

$$
\begin{aligned}
\varepsilon_+ &= \frac{1}{2}\left(\varepsilon_{xx} + \varepsilon_{yy}\right) + i\varepsilon_{xy} = R - \rho n_\perp^2 \\
\varepsilon_- &= \frac{1}{2}\left(\varepsilon_{xx} + \varepsilon_{yy}\right) - i\varepsilon_{xy} = L - \lambda n_\perp^2 \\
\varepsilon_\wedge &= \frac{1}{2}\left(\varepsilon_{xx} - \varepsilon_{yy}\right) = -\varepsilon n_\perp^2
\end{aligned}
\tag{10}
$$

so that

$$S = \frac{1}{2}(R+L) \qquad D = \frac{1}{2}(R-L)$$

(11)

$$\sigma_1 = \frac{1}{2}(\rho+\lambda) + \tau \qquad \sigma_2 = \frac{1}{2}(\rho+\lambda) - \tau$$

$$\delta = \frac{1}{2}(\rho-\lambda)$$

Capital letters are used for the terms which remain finite in the limit of zero Larmor radius. Well outside the Doppler broadened resonances,

$$\left| \frac{\omega - n\Omega_{\alpha i}}{k_{//} v_{thi}} \right| >> 1 \qquad n = 0, \pm 1 \tag{12}$$

they reduce to the elements of the cold plasma dielectric tensor as derived by Stix /1/. We find it convenient to retain Stix notations for these quantities modified to take into account the Cerenkov and cyclotron resonances. Small greek letters are used for the finite Larmor radii contributions. The explicit form of the quantities appearing in Eqs. (9) and (10) is:

$$R = 1 - \sum_j \frac{\omega_{pj}^2}{\omega^2}\left(-x_{0j} Z(x_{-1j})\right) \tag{13}$$

$$L = 1 - \sum_j \frac{\omega_{pj}^2}{\omega^2}\left(-x_{0j} Z(x_{1j})\right)$$

$$P = 1 - \sum_j \frac{\omega_{pj}^2}{\omega^2} x_{0j}^2 Z'(x_{0j})$$

$$\rho = \frac{1}{2}\sum_j \frac{\omega_{pj}^2}{\Omega_{cj}^2}\frac{v_{thj}^2}{c^2}\left[\left(-x_{0j} Z(x_{0j})\right) - 2\left(-x_{0j} Z(x_{-1j})\right) + \left(-x_{0j} Z(x_{-2j})\right)\right]$$

$$\lambda = \frac{1}{2}\sum_j \frac{\omega_{pj}^2}{\Omega_{cj}^2}\frac{v_{thj}^2}{c^2}\left[\left(-x_{0j} Z(x_{0j})\right) - 2\left(-x_{0j} Z(x_{1j})\right) + \left(-x_{0j} Z(x_{2j})\right)\right]$$

$$\tau = \frac{1}{2}\sum_j \frac{\omega_{pj}^2}{\Omega_{cj}^2}\frac{v_{thj}^2}{c^2}\left[-\left(x_{0j}Z(x_{0j})\right)+\frac{1}{2}\left[\left(-x_{0j}Z(x_{-1j})\right)+\left(-x_{0j}Z(x_{+1j})\right)\right]\right]$$

$$\sigma_1 = \frac{1}{2}\sum_j \frac{\omega_{pj}^2}{\Omega_{cj}^2}\frac{v_{thj}^2}{c^2}\left\{-\frac{1}{2}\left[\left(-x_{0j}Z(x_{-1j})\right)+\left(-x_{0j}Z(x_{+1j})\right)\right]+\right.$$
$$\left.+\frac{1}{2}\left[\left(-x_{0j}Z(x_{-2j})\right)+\left(-x_{0j}Z(x_{+2j})\right)\right]\right\}$$

$$\eta = \frac{1}{4}\sum_j \frac{\omega_{pj}^2}{\omega\Omega_{cj}}\frac{v_{thj}^2}{c^2}\left[x_{0j}^2Z'(x_{-1j})-x_{0j}^2Z'(x_{+1j})\right]$$

$$\xi = \frac{1}{2}\sum_j \frac{\omega_{pj}^2}{\omega\Omega_{cj}}\frac{v_{thj}^2}{c^2}\left[x_{0j}^2Z'(x_{0j})-\left(x_{0j}^2Z'(x\ )+x_{0j}^2Z'(x_{+1j})\right)\right]$$

$$\pi = \frac{1}{2}\sum_j \frac{\omega_{pj}^2}{\Omega_{cj}^2}\frac{v_{thj}^2}{c^2}\left\{-x_{0j}^2Z'(x_{0j})+\right.$$
$$\left.+\frac{1}{2}\left[\frac{\omega+\Omega_j}{\omega}x_{0j}^2Z'(x_{-1j})+\frac{\omega-\Omega_j}{\omega}x_{0j}^2Z'(x_{+1j})\right]\right\}$$

To first order in $k_\perp^2\rho_i^2/2$ the dispersion relation becomes a cubic equation for $n_\perp^2$:

$$H = -\sigma_1 n_\perp^6 + A n_\perp^4 - B n_\perp^2 + C = 0 \qquad (14)$$

where

$$A = S + \alpha$$
$$B = RL + PS - n_{/\!/}^2(P+S) + \beta \qquad (15)$$
$$C = P(n_{/\!/}^2 - R)(n_{/\!/}^2 - L$$
$$\alpha = -(n_{/\!/}^2 - S)(\sigma_1+\sigma_2+\pi) + n_{/\!/}^2(\sigma_2+2\eta) - 2D\delta + P\sigma_1$$
$$\beta = \pi(n_{/\!/}^2 - R)(n_{/\!/}^2 - L) - P\left[(n_{/\!/}^2 - S)(\sigma_1+\sigma_2)+2D\delta\right]$$
$$+2n_{/\!/}^2\left[D\delta-(n_{/\!/}^2-S)\eta\right]$$

b) Small electron inertia development

As a consequence of the large value of the mass ratio $M = m_i/m_e$, the coefficients of Eq. (14) differ widely in order of magnitude. To make the best use of this fact, let us note that in the ion frequency domain

$$\omega/\Omega_{ci} = O(1) \qquad \omega/\Omega_{ce} = O(M^{-1}) \tag{16}$$

$$\omega_{pi}^2/\omega^2 = O(M) \qquad \omega_{pe}^2/\omega^2 = O(M^2)$$

Moreover

$$\frac{v_{the}^2}{c^2} = \frac{T_e}{255} \qquad \frac{v_{thi}^2}{c^2} = \frac{T_i}{255 \cdot M} \tag{17}$$

(temperatures in Kev) are also very small, respectively $O(M^{-1})$ and $O(M^{-2})$ in order of magnitude. The parallel index $n_{//}$ can take any value between zero and a few units. Indeed if

$$n_{//}\sqrt{T_e} \gg 1 \tag{18}$$

damping by the electrons (electron transit time pumping and to a smaller extent electron Landau damping) sets in, and the waves cannot be made to penetrate freely into the plasma core (the increasing optical thickness of the evanescence layer between the antenna and the R cut-off near the plasma edge also makes coupling of waves with large $n_{//}$ less effective).

The leading terms of the coefficients in Eq. (14) are ordered as successive powers of M as follows:

$$\sigma_1 : A : B : C = M^{-1} : M : M^2 : M^3 \tag{19}$$

With the above estimates it is easily seen that among the finite Larmor radius terms, only σ_1 has to be retained, both in the coefficient of $n_\perp^6$, where it appears alone, and in the coefficient of $n_\perp^4$, where it is multiplied by the very large factor $P = -\omega_{pe}^2/\omega^2$ (the fact that the finite temperature corrections to σ_1 play such a dominant role is related to the transversality of rotrot $(\vec{E}) = -\vec{k} \times (\vec{k} \times \vec{E})$). We are thus led to the following approximate dispersion relation:

$$H = -\sigma_1 n_\perp^6 + A n_\perp^4 - B n_\perp^2 + C = 0 \tag{20}$$

$$A = S + P\sigma_1$$

$$B = -P\left\{(n_{//}^2 - S) + (n_{//}^2 - R)\lambda + (n_{//}^2 - L)\varrho\right\}$$

$$C = P(n_{//}^2 - R)(n_{//}^2 - L)$$

where

$$R = 1 + \frac{\omega_{pe}^2}{\Omega_{ce}^2} - \sum_j \frac{\omega_{pj}^2}{\omega^2}\left[\frac{\omega}{\omega + \Omega_j} - \frac{\omega}{\Omega_j}\right] \tag{21}$$

$$L = 1 + \frac{\omega_{pe}^2}{\Omega_{ce}^2} - \sum_j \frac{\omega_{pj}^2}{\omega^2}\left[-x_{0j} Z(x_{1j}) + \frac{\omega}{\Omega_j}\right] .$$

$$P = -\frac{\omega_{pe}^2}{\omega^2} x_{0e}^2 Z'(x_{0e})$$

$$\sigma_1 = \sigma_e + \frac{1}{2}(\varrho + \lambda) + \tau$$

$$\sigma_e = \frac{3}{8}\frac{\omega_{pe}^2}{\Omega_{ce}^2}\frac{v_{the}^2}{c^2}$$

$$\varrho = \frac{1}{2}\sum_j \frac{\omega_{pj}^2}{\Omega_{cj}^2}\frac{v_{thj}^2}{c^2}\left[1 - 2\frac{\omega}{\omega + \Omega_j} + \frac{\omega}{\omega + 2\Omega_j}\right]$$

$$\lambda = \frac{1}{2} \sum_j \frac{\omega_{pj}^2}{\Omega_{cj}^2} \frac{v_{thj}^2}{c^2} \left[1 - 2\left(-x_{0j} Z(x_{1j})\right) + \left(-x_{0j} Z(x_{2j})\right) \right]$$

$$\varepsilon = \frac{1}{2} \sum_j \frac{\omega_{pj}^2}{\Omega_{cj}^2} \frac{v_{thj}^2}{c^2} \left[-1 + \frac{1}{2}\left(\left(-x_{0j} Z(x_{1j})\right) + \frac{\omega}{\omega + \Omega_j}\right) \right]$$

Here the summation extends on the ions only: in R and L we have expanded the electron contribution in ω/Ω_e to second order (retaining successively the contributions from the $\vec{E} \times \vec{B}$ drift and the polarization drift of the electrons), and used charge neutrality,

$$\frac{\omega_{pe}^2}{\omega \Omega_e} = \sum_j \frac{\omega_{pj}^2}{\omega \Omega_{cj}} \tag{22}$$

According to above considerations, the finite Larmor radius terms in coefficient B give a negligible correction to the roots of Eq. (20), with one exception, however. As discussed in section 4, they become important in the vicinity of the first harmonic $\omega = 2\Omega_{cj}$, where they are resonant, while the cold-plasma terms remain finite. In all other cases they can be safely neglected.

c) Polarization

Before discussing qualitatively the roots of Eq. (20), it is useful to obtain expressions for the polarizations. To this end it is convenient to decompose the perpendicular electric field into circularly polarized, rather than plane polarized, components:

$$E_\pm = \frac{1}{\sqrt{2}} \left(E_x \mp i E_y \right) \tag{23}$$

They have to satisfy

$$\sum_j M_{ij} E_j = 0 \qquad i = 1,2,3 \tag{24}$$

$$\left(E_1 = E_+,\ E_2 = E_-,\ E_3 = E_z\right)$$

where

$$M_{ij} = \begin{vmatrix} \frac{1}{2}(\varepsilon_{xx}+\varepsilon_{yy}) - i\varepsilon_{xy} - n_{//}^2 - \frac{1}{2}n_\perp^2 & \frac{1}{2}(\varepsilon_{xx}-\varepsilon_{yy}) + \frac{1}{2}n_\perp^2 & \frac{1}{2}n_\perp n_{//} \\ \frac{1}{2}(\varepsilon_{xx}-\varepsilon_{yy}) + \frac{1}{2}n_\perp^2 & \frac{1}{2}(\varepsilon_{xx}+\varepsilon_{yy}) + i\varepsilon_{xy} - n_{//}^2 - \frac{1}{2}n_\perp^2 & \frac{1}{2}n_\perp n_{//} \\ \frac{1}{2}n_\perp n_{//} & \frac{1}{2}n_{//} n_\perp & \varepsilon_{zz} - n_{//}^2 \end{vmatrix} = \tag{25}$$

$$= \begin{vmatrix} L - n_{//}^2 - \left(\frac{1}{2}+\lambda\right)n_\perp^2 & \left(\frac{1}{2}-\zeta\right)n_\perp^2 & \frac{1}{2}n_{//} n_\perp \\ \left(\frac{1}{2}-\zeta\right)n_\perp^2 & R - n_{//}^2 - \left(\frac{1}{2}+\rho\right)n_\perp^2 & \frac{1}{2}n_\perp n_{//} \\ \frac{1}{2}n_\perp n_{//} & \frac{1}{2}n_\perp n_{//} & P - n_\perp^2 \end{vmatrix}$$

Let m_{ij} be the minor corresponding to the element M_{ij} of the above matrix. Then

$$\sum_k m_{jk} M_{ki} = 0 \qquad i,j = 1,2,3 \tag{26}$$

because of the dispersion relation. Hence, for any choice of the line i, Ej will be proportional to m_{ij}.

Introducing as usual the unitary polarization vector $\vec{e}$ such that

$$\vec{e}^{*} \cdot \vec{e} \equiv 1 \qquad \vec{E} = |E|\,\vec{e} \tag{27}$$

and using the third line, we have:

$$e_{+} = K\, n_{\perp} n_{/\!/} \left[R - (P-S) n_{\perp}^{2} - n_{/\!/}^{2} \right]$$

$$e_{-} = K\, n_{\perp} n_{/\!/} \left[L - (\lambda - S) n_{\perp}^{2} - n_{/\!/}^{2} \right] \tag{28}$$

where K is the normalization constant. This procedure would express the parallel component of the electric field as the difference of two very large and almost equal quantities. Instead, we use again (25) to obtain

$$e_{z} = -\frac{1}{2} n_{\perp} n_{/\!/} \frac{e_{+} + e_{-}}{P - n_{\perp}^{2}} =$$

$$= -K n_{\perp}^{2} n_{/\!/} \frac{S - \sigma n_{\perp}^{2} - (n_{\perp}^{2} + n_{/\!/}^{2})}{P - n_{\perp}^{2}} \tag{29}$$

The screening of the parallel electric field by the electrons makes $|e_{z}| = O\,(m_{e}/m_{i})$, as apparent from this equation.

d) Waves in the ion cyclotron frequency range

The approximated dispersion relation (20) describes three plasma waves. The smallest root is the fast, or extraordinary wave, also known as the compressional Alfwen wave. It is this wave which is normally excited by external antennas in large Tokamaks.

Its dispersion relation is accurately approximated by the expression

(30) $$n_\perp^2 = - \frac{(n_{//}^2 - R)(n_{//}^2 - L)}{(n_{//}^2 - S)}$$

The other two waves are the slow, or ordinary wave, and a hot-plasma wave, which receives different names depending on the parameter range which is investigated. We must generally distinguish two situations, depending on the value of β (ratio between kinetic and magnetic pressure). At very low β,

(31) $$\beta = \frac{8\pi n T}{B_0^2} \ll \frac{m_e}{m_i}$$

the slow wave has the approximate dispersion relation

(32) $$n_\perp^2 = - (n_{//}^2 - S) \frac{P}{S}$$

and the hot plasma wave

(33) $$n_\perp^2 = \frac{S}{\sigma_1}$$

In the ion cyclotron frequency range $|P|$ is so large that in practice Eq. (32) makes sense only if

(34) $$n_{//}^2 = S$$

The wave satisfying this dispersion relation is known as the torsional Alfven wave below the ion cyclotron frequency, and as the Ion Cyclotron wave near the cyclotron frequency; it displays the well known parallel resonance ($n_{//}^2 \to \infty$) when $\omega \to \Omega_i$ from below, which is exploited in the "magnetic beach" configuration /1/, not easily realizable in a Tokamak.

At low frequencies, $\omega \ll \Omega_i$, Eq. (33) is the dispersion relation of the ion sound wave,

(35) $$\omega^2 = k_\perp^2 \rho_i^2 v_{thi}^2$$

The condition $k_\perp^2 \rho_i^2 \ll 1$ is however no longer satisfied by this root when ω is of the order of Ω_i. Then Eq. (33) is actually accurate only in the vicinity of the points where σ_1 becomes large, namely near $\omega = 2\Omega_i$ where Eq. (33) describes the first Ion Berstein wave, or where S becomes very small, namely in the vicinity of the Two-Ion Hybrid resonances described in the next section.

In large tokamaks with central temperatures approaching or above one Kev, however, condition (31) is usually violated by a considerable margin, even near the plasma periphery. Thus we are more interested in the opposite situation, in which

(36) $$\beta \gtrsim \frac{m_e}{m_i}$$

In this case the approximate dispersion relations are respectively for the slow wave

(37) $$n_\perp^2 = P = -\frac{\omega_{pe}^2}{\omega^2}$$

and for the hot plasma wave

(38) $$n_\perp^2 = -\left(n_{//}^2 - S\right)/\sigma_1$$

In spite of the fact that Eqs. (37) and (38) coincide with Eqs. (32) and (33) at perpendicular propagation, they imply a different physics in a non-uniform plasma near the critical points where confluences between different branches occurs (i.e. near $\omega = 2\Omega_i$ and where S = 0).

The slow wave is always evanescent, with an exceedingly short evanescence length, and never couples to the other two waves. This is due to the effective screening of the electric field parallel to B_o, as mentioned after Eq. (29). For all purposes, under condition (36), we can ignore this wave inside the plasma altogether. It can however affect coupling of the waves by external antennas, since it implies the exitation of a sheath of image currents along the static magnetic field on the surface of the plasma if the corresponding component of the electric field of the antenna is not properly shielded.

At low frequencies, Eq. (38) is essentially identical with Eq. (33) above, and again describes the ion sound wave. The only exception occurs when

$$n_{//}^2 = S \qquad \text{or} \qquad k_{//}^2 v_A^2 = \omega^2 \tag{39}$$

$$v_A^2 = c^2 \cdot \frac{\Omega_{ci}^2}{\omega_{Pi}^2} = \left(\frac{4\pi m_i n_i c^2}{B_o^2} \right)^{-1}$$

happens to be satisfied; this wave is then known as the Kinetic Alfven wave. In the ion cyclotron frequency range the hot plasma wave (38) is known as the first Ion Berstein wave (higher Berstein waves would be introduced by retaining higher order terms in the $k^2 \varrho_i^2$ expansion of the dispersion relation; contrary to the first one, however, the n-th Bernstein wave can propagate only in a neighborhood of the corresponding harmonic of the ion cyclotron frequency, unless the density happens to correspond to the Lower Hybrid resonance near the harmonic in question).

Since the slow plasma wave (37) is essentially of no interest, when (36) is satisfied we can simplify further the dispersion relation by neclecting the electron inertia altogether:

$$H = \sigma_1 n_\perp^4 + \left[(n_{//}^2 - S) + \beta \right] n_\perp^2 + (n_{//}^2 - R)(n_{//}^2 - L) = 0 \tag{40}$$

$$\beta = (n_{//}^2 - R)\lambda + (n_{//}^2 - L) \cdot \varrho$$

This form, which describes adequately both the fast wave and the ion Bernstein wave, will be mainly used in the following. For these two waves, a comparison of the results from (40) and from (20) shows that the difference never exceeds a few parts in a thousand.

A summary of the results of this section is given in Table 1.

TABLE 1

Approximate root	$\omega \ll \Omega_{ci}$	$\omega \sim O(\Omega_{ci})$	$\omega \cong 2\Omega_{ci}$	$\omega \gg \Omega_{ci}$
$n_\perp^2 = -\dfrac{(n_{\parallel}^2 - R)(n_{\parallel}^2 - L)}{(n_{\parallel}^2 - S)}$	Compressional Alfven Wave $k^2 v_A^2 = \omega^2$	Fast wave	Fast wave (has a confluence with the Ion Bernstein wave)	Fast wave
$n_\perp^2 =$ $(n_{\parallel}^2 - S)(-P/S)$ (if $\beta \ll m_e/m_i$ or $\omega \gg \Omega_{ci}$	Torsional Alfven wave $k_{\parallel}^2 v_A^2 = \omega^2$	Ion cyclotron wave (exhibits the parallel resonance at $\omega = \Omega_{ci}$)	Ion cyclotron wave	Lower Hybrid wave $\dfrac{k_\perp^2}{k_{\parallel}^2} \simeq \dfrac{m_i}{m_e} \dfrac{\omega_{LH}^2}{\omega^2 - \omega_{LH}^2}$
$-P$ (otherwise)	Evanescent	Evanescent	Evanescent	Quasi-electrostatic
$n_\perp^2 =$ S/σ_1 (if $\beta \ll m_e/m_i$ or $\omega \gg \Omega_{ci}$	Acoustic wave $k_\perp^2 v_{thi}^2 = \omega^2$ (Quasi-electrostatic)	$k_\perp^2 \rho_i^2 \gtrsim 1$	First Ion Bernstein wave $k_\perp^2 v_{thi}^2 \approx \frac{1}{3}(2\Omega_{ci} - \omega)$	Evanescent until the perpendicular lower Hybrid Resonance $S = 0$
$-(n_{\parallel}^2 - S)/\sigma_1$ (otherwise)	Kinetic Alfven wave if $k_{\parallel}^2 v_A^2 = \omega^2$ otherwise Acoustic wave as above			

3. CUT-OFFS AND RESONANCES

We define a cut-off as a zero of the perpendicular index. This is not the definition used in an infinite, homogeneous plasma /1/; it is however the appropriate one in the present geometry. A cut-off will separate a region of propagation from a region of evanescence, so that a wave impinging on it will suffer total or partial reflection there, depending on the optical thickness of the evanescence layer on the other side. The fast wave encounters a cut-off when either

$$n_{//}^2 = R \quad \text{or} \quad n_{//}^2 = L \tag{41}$$

In the approximation (30), on the other hand, the surfaces where

$$n_{//}^2 = S \tag{42}$$

appear as resonances of the fast wave (infinities of the perpendicular index). Actually, of course, near such a surface, Eq. (30) no longer holds: what happens is that the index of the fast wave increases, and the index of the slow cold-plasma wave (32) or of the hot-plasma wave (38) (depending on the value of β) decreases, so that a confluence takes place. A true resonance in the present sense can only occur where S = 0 in a cold plasma (lower, upper, and two-ion hybrid): when hot plasma effects are taken into account, such a resonance goes over into a confluence of the cold-plasma wave with a much slower hot-plasma wave. Since this is just the behaviour of the fast wave at low frequency ($\omega \sim \Omega_i$) when Eq. (42) is satisfied, this extension of the definition of resonance appears perfectly justified.

The importance of locating cut-offs and resonances for the study of coupling, propagation and absorption is obvious. It is convenient to discuss separately the behaviour near the plasma edge (low density), and the behaviour in the plasma core (large density).

A) Low-density cut-offs and resonances

The behaviour at very low density does not depend on the plasma composition, so that it will suffice to consider a single species of ions with $m_i/m_e = M$. Figs. 1a and 1b show the cold dielectric tensor elements R, L and S versus density for $\omega < \Omega_{ci}$ and for $\omega > \Omega_{ci}$ respectively.

According to Fig. 1a, at frequencies lower than the ion cyclotron frequency, waves with $n_{//}^2 < 1$ penetrate into the plasma without encountering any cut-off or resonance. Waves with $n_{//}^2 > 1$, on the other hand, which are evanescent in vacuum, encounter first a L-cut-off, then propagate to the a resonance, are again evanescent between this resonance and the R-cut-off, and propagate finally into the plasma. The resonance encountered by these waves is actually a confluence with the slow cold-plasma wave (31), since we are considering here very low densities ($\beta \lesssim M^{-1}$). It is a limiting case of an "Alfven resonance".

According to Fig. 1b, at frequencies above the ion cyclotron frequency, waves with $n_{//}^2 < 1$ become evanescent at a L-cut-off, then tunnel to a resonance, beyond which they propagate again towards the plasma core. Waves with $n_{//}^2 > 1$ on the other hand remain evanescent up to the R-cut-off, and propagate at higher densities. The resonance encountered in this case by the waves with $n_{//}^2 < 1$ is again a confluence with the slow cold-plasma wave (31); in this case however the latter proceeds to a true cold plasma resonance (S = 0), which is the limit of the Lower Hybrid resonance at frequencies approaching Ω_i (the condition $n_{//}^2 > 1$ for the absence of this confluence is the 'accessibility condition' of the L.H. resonance in the same limit).

When applied to the perifery of a Tokamak plasma, however, the above description cannot be taken literally. Indeed, for all but unreasonably large values of $n_{//}^2$, all the cut-off and resonances mentioned above are confined to densities about m_e/m_i smaller than the central density, i.e. of the order of 10^{10} to 10^{11} cm^{-3}.

A layer of such low density is not well defined, and in any case much thinner than the local wavelength (still essentially identical with the vacuum wavelength). A more appropriate model of the plasma periphery would assume a vacuum layer, through which waves with $n_{//}^2 > 1$ must tunnel, followed by a suitable low density plasma in which all waves are propagating. In such a model the 'resonances' described above should appear as induced surface currents. An evaluation of the impedance and power spectre of the antenna including the effect of dissipation of these currents is not yet available.

B) Ion Hybrid resonances

In the ion cyclotron frequency range, and for the plasma parameters typical of tokamaks, no cut-off or resonances other than those mentioned above can occur in a single species plasma. On the other hand, if more species of ions with different Z/A ratios are present, an L-cut-off and a resonance occur between each couple of cyclotron resonances. The importance of the Two-Ion-Hybrid resonance is well-known /3/. In this section we will give the general formulae to locate these singularities; the behaviour of the perpendicular index in their neighborhood taking into account temperature effects will be described on the basis of two typical examples in the next section. Here we will only note that since these resonances are normally located in plasmas with $\beta \gtrsim m_e/m_i$, they always couple the fast wave (30) with the hot plasma Ion Bernstein wave (38).

Due to the fact that in a typical tokamak plasma $\omega_{pi}^2/\Omega_{ci}^2 = O(M)$, the position of the Two Ion Hybrid resonance $n_{//}^2 = S$ and of the cut-off $n_{//}^2 = L$ can be assimilated, with an accuracy of the order of $1/M$, with the positions where $S-1 = 0$ and $L-1 = 0$, respectively. In particular, then, they are independent from the value of $n_{//}^2$, provided of course that $n_{//}^2 \ll M$.

Let $\nu_i = n_i/n_e$, Z_i, and A_i, $i = 1,2$, be the concentrations, atomic charges and masses, of the two ions.

We first express the position of the singularities in a symmetric form, through the value of the magnetic field where they occur. For the cut-off we have:

$$\left.\frac{\omega}{\Omega_{cH}}\right)_{c.o.} = Z_1 Z_2 \left(\frac{\nu_1}{A_2} + \frac{\nu_2}{A_1}\right) \tag{43}$$

and for the resonance we have:

$$\left.\frac{\omega^2}{\Omega_c^2}\right)_{Res} = \frac{\nu_1 Z_1 \frac{Z_2}{A_2} + \nu_2 Z_2 \frac{Z_1}{A_1}}{\nu_1 Z_1 \frac{A_2}{Z_2} + \nu_2 Z_2 \frac{A_1}{Z_1}} \tag{44}$$

(here Ω_{cH} is the cyclotron frequency of protons). In most cases, however, a "minority" concentration of one species, say species 2, is present in a plasma essentially composed of species 1. Both the resonance and the cut-off approach the cyclotron resonance of the minority species when its concentration decreases to zero. Using charge neutrality,

$$\sum \nu_i Z_i = 1 \tag{45}$$

we can rewrite Eqs. (43) and (44) in a form that makes this fact explicit:

$$\left.\frac{\omega}{\Omega_{c2}}\right)_{c.o} = 1 + \nu_2 Z_2 \left(\frac{Z_1/A_1}{Z_2/A_2} - 1\right) \tag{46}$$

and

$$\left.\frac{\omega^2}{\Omega_{c2}^2}\right)_{Res} = \frac{1 + \nu_2 Z_2 \left(\frac{Z_1/A_1}{Z_2/A_2} - 1\right)}{1 + \nu_2 Z_2 \left(\frac{A_1/Z_1}{A_2/Z_2} - 1\right)} \tag{47}$$

If the poloidal magnetic field is disregarded, and R_0 denotes the major radius at which the fundamental cyclotron resonance of the minority species is located, the position of the singularities is given by

$$\left(\frac{\Delta R}{R_0}\right)_{c.o} = \nu_2 Z_2 \left(\frac{Z_1/A_1}{Z_2/A_2} - 1\right) \tag{48}$$

and

$$\left(\frac{\Delta R}{R_0}\right)_{c.o} = \sqrt{\frac{1+\nu_2 Z_2\left(\frac{Z_1/A_1}{Z_2/A_2}-1\right)}{1+\nu_2 Z_2\left(\frac{Z_2/A_2}{Z_1/A_1}-1\right)}} - 1 \tag{49}$$

Fig. 2 shows the cut-off and resonance in a Deuterium plasma with Hydrogen minority. In this case (minority species having Z/A greater than the main species) the Two Ion Hybrid resonance is located on the high magnetic field side of the Cyclotron resonance of the minority species. The vertical scale of Fig. 2 is labelled in cm., assuming the cyclotron resonance of hydrogen to be located at R_0 = 300 cm, on the magnetic axis of the JET plasma.

Fig. 3 shows the same plots in the case of a He_3^{++} minority in a Hydrogen plasma. In this case (minority species with the smallest Z/A ratio) the Two Ion Resonance is located on the low magnetic field side of the Cyclotron resonance of the minority ions.

4. DISPERSION DIAGRAMS NEAR RESONANCES

In this section we discuss in more details the behaviour of the dispersion relation near the resonances discussed in the previous section. The examples which will be presented have been obtained for a plasma of the JET size (toroidal radius, characterizing here the gradient of magnetic field intensity, R_0 = 3 m ; plasma radius a = 1.2 m). The central density is assumed to be $n_e = 8.0 \cdot 10^{13}$ cm^{-3}, the central temperatures, unless otherwise stated, T_{i_0} = 1 Kev and T_{e_0} = 1.2 Kev.

Approximately parabolic profiles have been assumed; the density and temperature variations in the region of interest are usually quite small, however: the variation of refractive index is mainly attributable to the gradient of the static magnetic field.

A) First Harmonic Heating of a single species plasma

The simplest situation of interest is heating at the first harmonic of the ion cyclotron resonance in a single species plasma. In the numerical examples we have assumed this species to be Deuterium, so that this situation is also the limiting case of a D - H mixture, heated by exploiting the Two-Ion-hybrid Resonance, when the concentration of Hydrogen vanishes. Scaling to other plasmas, in particular to pure Hydrogen (a more likely candidate for first harmonic heating in JET), is however immediate.

Fig. 4 shows $n_\perp^2$ versus position for the case $n_{//} = 0$. The resonance $\omega = 2\Omega_D$ is located on the magnetic axis (R = 3 m) and the distance X from this axis is given in cm, with the low field side to the right (positive X). The main feature of this figure is the evanescence layer just to the left of the first harmonic resonance, in which the two roots for $n_\perp^2$ are complex conjugate. The existence of this evanescence layer was first noted by Weynants /4/.

The confluences between the fast wave (branches labelled 'F' in Fig. 4 and the Ion Bernstein wave (branches labelled 'B') in this case is not due to a 'resonance' in the sense of the previous section (S = 0), but to the fact that, in the limit of perpendicular propagation, σ_1 becomes infinite as Ω_D approaches $\omega/2$. It is indeed the relatively large value of σ_1 here that is responsible for the existence of the first Bernstein wave near $\omega = 2\Omega_D$ to begin with. The confluence between this wave and the fast wave in the vicinity of the first harmonic resonance can be easily predicted from Eqs. (30) and (38) of Section 2, with considerations similar to those used in Section 4 to locate the two-ion-hybrid resonances and cut-offs.

The width of the evanescence layer is easily deduced from the approximate dispersion relation for quasi-perpendicular incidence,

$$\sigma_1 n_\perp^4 - \left(S + R\lambda + L\varrho\right) n_\perp^2 + RL = 0 \tag{50}$$

where, near $\Omega = \omega/2$

$$\sigma_1 \cong \frac{1}{2}\lambda \cong \frac{1}{4}\frac{\omega_{PD}^2}{\Omega_{cD}^2}\frac{v_{thD}^2}{c^2}\left(-x_{0D}Z(x_{1D})\right) \tag{51}$$

$$\approx \frac{1}{4}\beta_D \frac{\omega}{\omega - 2\Omega_D} \approx \frac{1}{4}\beta_D \frac{R_0}{X}$$

$$\varrho \approx \tau \approx 0$$

$$R \approx \frac{1}{3}\frac{\omega_{PD}^2}{\Omega_{cD}^2} \qquad L \approx -\frac{\omega_{PD}^2}{\Omega_{cD}^2}$$

The discriminant of Eq. (50),

$$\Delta = \left(S + R\lambda + L\varrho\right)^2 - 4RL\sigma_1 \approx \tag{52}$$

$$\approx \frac{1}{9}\frac{\omega_{PD}^2}{\Omega_{cD}^2}\left(\lambda^2 + 4\lambda + 1\right)$$

is negative when $-2-\sqrt{3} < \lambda < -2+\sqrt{3}$, i.e.:

$$-2\left(2+\sqrt{3}\right)\beta_i < \frac{X}{R_0} < -2\left(2-\sqrt{3}\right)\beta_i \tag{53}$$

Here $\beta_D = \beta T_D/(T_D + T_e)$ is the ion contribution to the β of the plasma, and R_0 denotes the position of the first harmonic resonance. The negative sign in Eq. (53) means that the evanescence layer is on the high magnetic field side of the resonance, as already noted.

The optical thickness of the evanescence layer (number of e-folding lengths) can be easily estimated to be /5/:

(54) $$\eta_{OPT} = \frac{\pi}{2} \frac{\omega_{PD}}{c} R_0 \cdot \beta_D$$

With the JET parameters of the figure, η_{OPT} is about 0.2, and would reach unity at T_i = 5 kev; this implies that little power can be tunneled to the high magnetic field side, even if absorption in a single transit through the resonance is not complete (we will not try to estimate absorption in the present note). This is not a drawback, however, since waves launched from the low magnetic field side encounter first the cyclotron resonance.

It is worth noting here also that if the thermal corrections to the coefficient of $n_\perp^2$ where neglected in Eq. (40), the width of the evanescence region and its optical thickness would be overestimated by about a factor of 2. The reason is of course again the presence of the resonant terms in the finite-beta contributions, which are absent from the 'cold' part of the dielectric tensor. A further reason to keep these terms is that they are needed to ensure energy conservation when the problem of propagation in this region is studied using the ordinary differential equation ($ik_\perp \rightarrow$ d/dx) corresponding to the dispersion relation (50) /5/. The divergence of the lowest thermal corrections at $\omega = 2\Omega_i$, on the other hand, does not imply a breakdown of the $k_\perp^2 \rho_i^2$ development, since none of the higher terms neclected in obtaining Eq. (20) contains a resonant contribution at this point.

When $n_{//}$ is not zero, σ_- does not diverge at $\omega = \Omega_f/2$: its absolute value has a maximum at $|x_{2D}| \cong 2$, where

(55) $$\left| -x_{0D} Z(x_{2D}) \right| \approx 0.4 \frac{\omega}{k_{//} v_{thD}} \gg 1$$

If $-\lambda < 2 + \sqrt{3}$ at this point, the two roots miss each other. More important, for $|x_{2D}| \lesssim 2$, the imaginary part of Z cannot be neglected; in this region the two roots are no more complex conjugate, implying absorption simultaneously with evanescence. The width of the cyclotron absorption layer is given by:

(56) $$|\Delta X|_{Doppler} \approx 2\,|n_{//}|\,\frac{V_{thD}}{c}\,R_0$$

The layer where two complex conjugate roots exist will be completely washed out by the Doppler enlarged cyclotron resonance when

(57) $$|n_{//}| \gtrsim \frac{\omega_{PD}^2}{\Omega_{cD}^2}\,\frac{V_{thD}}{c} = \beta_D\,\frac{c}{V_{thD}}$$

The progressive merging of the absorption and evanescence regions with increasing $n_{//}$ is illustrated in Figs. 5 ($n_{//}$ = 1.5) and 6 ($n_{//}$ = 3). In the latter case condition (57) is already satisfied. In hydrogen, the transition to this situation occurs at a value of $n_{//}$ $\sqrt{2}$ times smaller for the same temperature, or at a lower temperature (by a factor 2) for a given $n_{//}$.

B) Hydrogen minority in a Deuterium plasma

As in the previous case, it is convenient to consider first the limit of perpendicular propagation. In the presence of a small concentration $\nu_H = n_H/n_e$ of Hydrogen ions, a new resonant term appears in the vicinity of the point where

(58) $$\omega = \Omega_H = 2\Omega_D$$

namely the fundamental resonance contribution to L from the minority species. This term, proportional to $\nu_H R_0/X$, makes L (and S) vanish, as discussed in Section 3, somewhat to the left (high magnetic field side) of the cyclotron resonance.

On the other hand, it is in competition with the first harmonic resonance terms in the finite-beta contributions due to Deuterium, proportional to β_D, and will therefore influence the location and separation of the confluences between the fast wave with the first Ion Bernstein wave.

In the approximate dispersion relation (50) in this case we can substitute:

(59) $$\lambda \cong \frac{1}{2}\beta_D \frac{R_0}{X} \qquad \rho \approx \xi \approx 0$$

$$R \cong \frac{1}{3}\frac{\omega_{PD}^2}{\Omega_{CD}^2} \qquad L \approx -\frac{\omega_{PD}^2}{\Omega_{CD}^2}\left(1 + \frac{1}{3}\nu_H \frac{R_0}{X}\right)$$

The confluences occur at the points where

(60) $$K^2\lambda^2 + 2(1+K)\lambda + 1 = 0$$

$$K = 1 + \frac{3\nu_H}{2\beta_D}$$

For vanishing H^+ concentration, K = 1, we recover the expression (54) as it should. As ν_H increases, the evanescence layer moves to the left, and its optical thickness increases. This is clearly shown by Figs. 7 (ν_H = 0., ν_H = 0.005, ν_H = 0.01) and 8 (ν_H = 0.05). A simple expression for the position and width of the layer can be obtained as soon as

(61) $$\nu_H \gg \beta_D$$

Then the centre of the evancescence layer is at

(62) $$X_{Evanesc.} \cong -\frac{3}{4}\nu_H R_0$$

($X_{Ev.}$ is always to the left, higher magnetic field side, of both the theoretical two-ion-hybrid cut-off and resonance). The width of the layer is:

$$(63) \qquad (\Delta X)_{Ev.} \cong \frac{3\sqrt{3}}{2} \nu_H \left(\frac{\nu_H}{\beta_D}\right)^{1/2} R_0$$

By comparing this with the distance of the center of the layer, $X_{Ev.}$ from the cut-off position, X_{CO} ,

$$(64) \qquad |X_{Ev} - X_{CO}| \approx \frac{1}{4} \nu_H R_0$$

it is immediately seen that the two-ion-hybrid cut-off L = 0 will be effectively present, and contribute to the thickness of the evanescence layer, as soon as condition (61) above is satisfied.

Cyclotron absorption of course sets in a finite $n_{//}$, and is confined to the layer (56) around X = 0. The condition for this layer to influence effectively the two-ion hybrid region is essentially the same as in the case of pure first harmonic heating as long as $\nu_H < \beta_D$, as illustrated by Fig. 9 ($\nu_H = 0.005$, $n_{//} = 1.5$ and $n_{//} = 3$). For higher 'minority' concentration, Doppler broadening will dominate if

$$(65) \qquad |n_{//}| \frac{v_{th\,i}}{c} \gtrsim \frac{3}{8} \nu_H$$

For a given $n_{//}$, this condition can be used to define a critical proton concentration, below which the dispersion curve is dominated by the majority species Hermitean contribution to the dielectric tensor, and by the Doppler-broadened resonance of the minority species ("minority heating" regime); above this critical concentration, on the other hand, the two-ion hybrid layer is well separated from the absorption layer ("ion hybrid" regime).

In a real set-up, this distinction is usually less clear-cut, since several $n_{//}$ are simultaneously excited as a rule; a rather broad transition will then separate the two regimes.

In the 'two-ion-hybrid' regime, the imaginary part of $n_\perp^2$ near the cyclotron resonances (58) is relatively small, as shown in Fig. 8 (in spite of the relatively large value of $n_{//}$). This does not mean small absorption, however: it is easily seen that the antihermitean part of the dielectric tensor is quite large, and the appropriate component of the electric field also appreciable there.

During heating, the minority species can acquire a temperature appreciably higher than the main ions. For completeness, Fig. 10 shows an example of dispersion relation in this case. If the heating rate is fast compared with the typical angle-scattering time, the distribution function of the minority ions can also be appreciably anisotropic, with $T_\perp$ larger than $T_{//}$. Contrary to a widespread belief, the dispersion relation (40) (or the more general one (20)) is perfectly adequate to deal with this situation, provided that $v_{th//} = (2T_{//}/m)^{1/2}$ is used in the argument of the Z's (parallel Doppler broadening) and $T_\perp$ is used elsewhere. Indeed, the corrections to R and L due to anisotropy of the distribution function, and not already included in Eq. (40), are easily shown to be

$$\delta L = \frac{1}{2}\sum_j \frac{\omega_{pj}^2}{\omega^2}\left(\frac{k_{//}^2 v_{thj}^2}{\omega^2}\right)\left(\frac{T_\perp}{T_{//}}-1\right) x_{0j}^2 Z'(x_{1j}) \tag{66}$$

$$\delta R = \frac{1}{2}\sum_j \frac{\omega_{pj}^2}{\omega^2}\left(\frac{k_{//}^2 v_{thj}^2}{\omega^2}\right)\left(\frac{T_\perp}{T_{//}}-1\right)\left(\frac{\omega}{\omega+\Omega_j}\right)^2$$

These are not only very small compared to R and L themselves, but are smaller than the finite Larmor radius corrections ϱ, λ and τ, by a factor $(k_{//}/k_\perp)^2 = O(m_e/m_i)$; hence they can be completely disregarded.

C) Helium-3 minority in an Hydrogen plasma

There is an essential difference between this heating scheme and the previous one, namely that the fundamental cyclotron resonance of the minority ions,

(67) $$\omega = \Omega_{cHe} = \frac{2}{3}\Omega_H$$

does not coincide with the firs harmonic for the main plasma. As a consequence, the hot-plasma wave in the vicinity of the Two-Ion-Hybrid resonance is not a Bernstein wave, but an acoustic wave with a much greater perpendicular index. In the absence of He ions, the dispersion relation of this wave is

(68) $$\omega^2 \approx 0{,}2\, k_\perp^2 v_{thH}^2$$

In the limit of perpendicular propagation in the presence of a small He_3^{++} concentration

(69) $$\nu_{He} = \frac{n_{He_3}}{n_e} \qquad \left(\frac{n_H}{n_e} = 1 - 2\nu_{He}\right)$$

we can substitute in Eq. (50) the approximate expressions

(70) $$\lambda \cong -\nu_{He}\beta_H \frac{R_0}{X} \qquad \sigma_1 \cong \frac{1}{4}\lambda$$

$$R \cong \frac{4}{15}\frac{\omega_{pH}^2}{\omega^2} \qquad L \cong \frac{4}{3}\frac{\omega_{pH}^2}{\omega^2}\left(1 - \frac{R_0}{X}\right)$$

The resonant terms in the cold-plasma contributions and in the finite Larmor radius contributions to the dielectric tensor are here proportional to each other, the latter being smaller by the very small factor $\nu_{He}\beta_H$: the term $R\lambda$ in the coefficient of $n_\perp^2$ can in particular be neglected.

It follows that the two roots of Eq. (50) exchange their role near the point where S = 0, as sketched in Fig. 11 a, and remain real throughout. Moreover, the value of $n_\perp^2$ at the resonance S = 0 is

$$(71) \qquad n_\perp^2 \Big)_{S=0} \cong \pm 0{,}5 \, \frac{\omega_{PH}^2}{\omega^2} \cdot \frac{1}{(\beta_H \nu_{He})^{1/2}}$$

i.e. $(\beta_H \nu_{He})^{-1/2}$ times larger than at the confluence with the Ion Bernstein wave in the case where the main ion species is near its own first harmonic cyclotron resonance. We may also note that the acoustic wave shows a 'resonance' (coupling with the slow cold-plasma wave) slightly to the left (high magnetic field side) of the Two-Ion-Resonance, where σ_i vanishes, and is propagating ($n_\perp^2 > 0$) everywhere else. Its perpendicular index, however, is so large, that the finite Larmor radius expansion is only marginally valid for this root, even at the point S = 0, where it is minimum, and certainly near the confluence with the slow wave.

It is therefore more appropriate in this case to neglect $\sigma_\perp$ altogether in Eq. (50), thus retaining only the fast wave,

$$(72) \qquad n_\perp^2 \cong RL/S$$

and to consider the Two-Ion-Resonance at S = 0 as a true singularity of the refractive index. Evanescence is then confined to the layer between the cut-off L = 0 and the resonance S = 0, and its optical thickness can be estimated to be /6/:

$$(73) \qquad \eta_{OPT} \cong \frac{\pi}{30} \, \frac{\omega_{PH}}{c} R_0 \nu_{He}$$

This point of view is confirmed by looking to the results for $n_{//} \neq 0$. The condition for cyclotron damping by He_3^{++} ions to influence the Two-Ion-Resonance can be written

$$(74) \qquad |n_{//}| \, \frac{v_{th\,He}}{c} \gtrsim \frac{1}{2} \nu_{He}$$

When this condition is satisfied, the dispersion curves behave as shown in Fig. 13 (γ_{ihe} = 0.025, $n_{//}$ = 0, 3, and 6). The 'singularity' of the $n_{//}$ = 0 case is replaced by a typical resonant curve with dissipation, low at $n_{//}$ = 3, more heavy at $n_{//}$ = 6. Throughout this region, the fast root is very well approximated (to within a few percent) by Eq. (30) of section 2, provided that L and S are given their complex value, as it should. Indeed, the He_3^{++} contributions to the dielectric tensor being complex, the approximate expression (30) will not diverge; as soon as condition (74) is satisfied, the two roots of Eq. (50) can no more exchange. The qualitative behaviour in this case is shown in Fig. 11 b.

When condition (74) is violated, the region of absorption is well separated from the Two-Ion Hybrid Resonance, and the latter retains its character of effective singularity of the fast wave (Fig. 13). For waves launced from the low magnetic field side of a Tokamak, as it is usually the case, the evanescence region associated with this cut-off resonance pair screens the absorption region. If the optical thickness (73) is not small, little heating can be achieved in this case. At the density of the examples, this limits the allowable concentration of He to one or two percent (since η_{opt} increases linearly with the plasma dimensions and with the square root of the density, this condition is much more severe in JET than in small tokamaks). In other words, in the case of He minority in a H plasma, efficient heating can be expected only in the true 'minority' regime.

Such a limitation in the allowable minority concentration is not encountered when He_3^{++} is added to Deuterium, since in this case the Hybrid layer is located beyond the cyclotron resonance of He. An example of this situation is illustrated in Fig. 14.

ACKNOWLEDGMENTS

Dr. M. Söll has run a code solving the complete dispersion relation (4) - (5) (with the sum over Bessel functions), allowing us a check of the accuracy of our approximate dispersion relations (20) and (40). In particular, this comparison was instrumental to understand the role of the finite Larmor radius corrections in the vicinity of the first harmonic of the cyclotron frequency.

We wish to thank also Dr. M. Ottaviani for checking part of the algebra and for useful comments.

REFERENCES

/1/ T. H. STIX: The Theory of Plasma Waves, McGraw-Hill, New York 1962

/2/ B. D. FRIED, S. D. CONTE: The Plasma Dispersion Function, Academic Press New York 1961

/3/ F. W. PERKINS: Nucl. Fusion 17, (1977), 1197

/4/ R. R. WEYNANTS: Phys. Rev. Lett. 33, (1974), 78.

/5/ D. G. SWANSON: Phys. Rev. Lett. 36, (1976), 316

/6/ Ref. /1/, Ch. 9.

FIGURE CAPTIONS

FIG. 1 - Qualitative behaviour of R, L, and S, near the plasma edge.

FIG. 2 - Position of the Two-Ion Hybrid resonance and cut-off versus plasma composition in a D-H plasma. Toroidal radius at the cyclotron resonance of H, R_o = 3 m.

FIG. 3 - Position of the Two-Ion Hybrid resonance and cut-off versus plasma composition in a H-He plasma. Toroidal radius at the cyclotron resonance of He, R_o = 3 m.

FIG. 4 - Perpendicular index squared versus position in a pure Deuterium plasma near the first harmonic of the Deuterium cyclotron resonance (at X = 0). n = 8 10^{13} T_i = 1 kev, T_e = 1.2 kev, B_o = 3.5 T at X = 0. Purely perpendicular incidence.

FIG. 5 - Same as Fig. 4, with $n_{//}$ = 1.5

FIG. 6 - Same as Fig. 4, with $n_{//}$ = 3.0

FIG. 7 - Perpendicular index squared versus position in a D-H plasma, for very small concentration of H. Purely perpendicular incidence. Other parameters as in Fig. 4.

FIG. 8 - Same as Fig. 7, with 5% of H. $n_{//}$ = 3.

FIG. 9 - Same as Fig. 7, with 0.5% of H (minority regime) for various values of $n_{//}$.

FIG. 10 - Same as Fig. 7, with 1% of H (minority regime), with T_D = 2 kev and T_H = 6 kev. Other parameters unchanged.

FIG. 11 - Qualitative behaviour of the fast and acoustic waves near the Two-Ion Hybrid resonance in a H-He plasma.

FIG. 12 - Perpendicular index of the fast wave near the Two-Ion Hybrid resonance in a H-He plasma, for very small concentration of He_3^{++} (0.5%), various $n_{//}$. Cyclotron resonance of He_3^{++} at X = 0. Other parameters as in Fig. 4.

FIG. 13 - Same as Fig. 12, with 2.5% of He_3^{++} .

FIG. 14 - Same as Fig. 12, with Deuterium instead of Hydrogen as majority species.

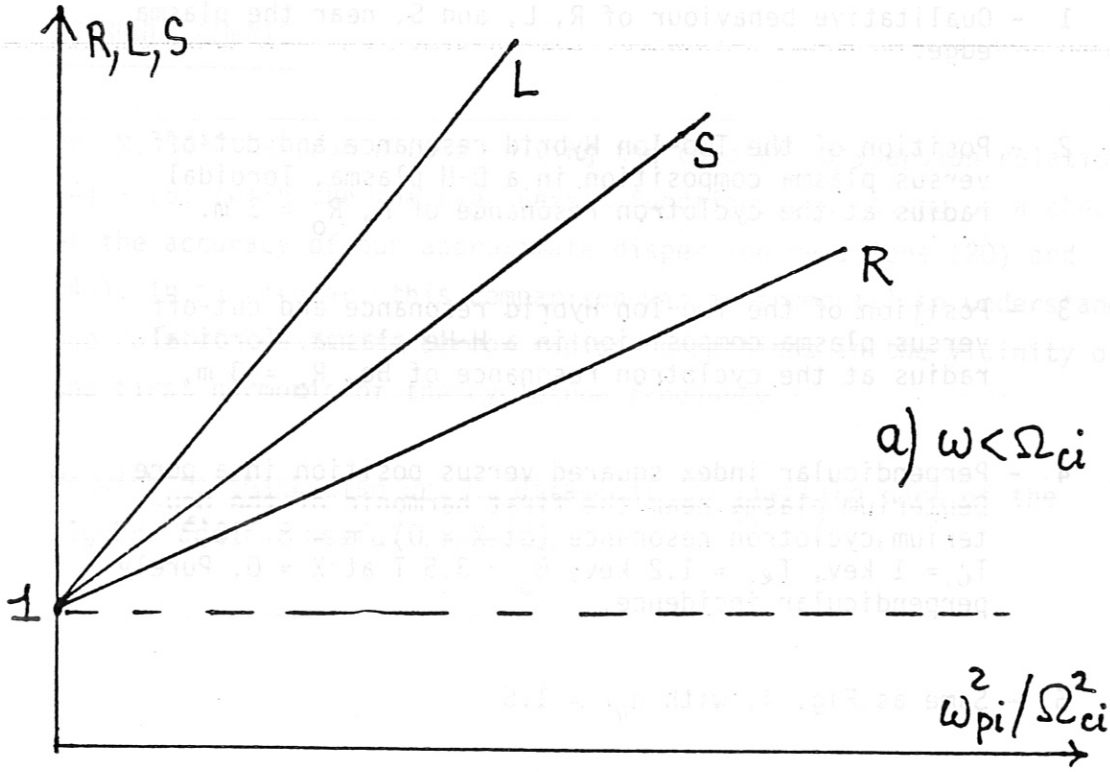
R,L,S
L
S
R
a) $\omega < \Omega_{ci}$
1
$\omega_{pi}^2/\Omega_{ci}^2$

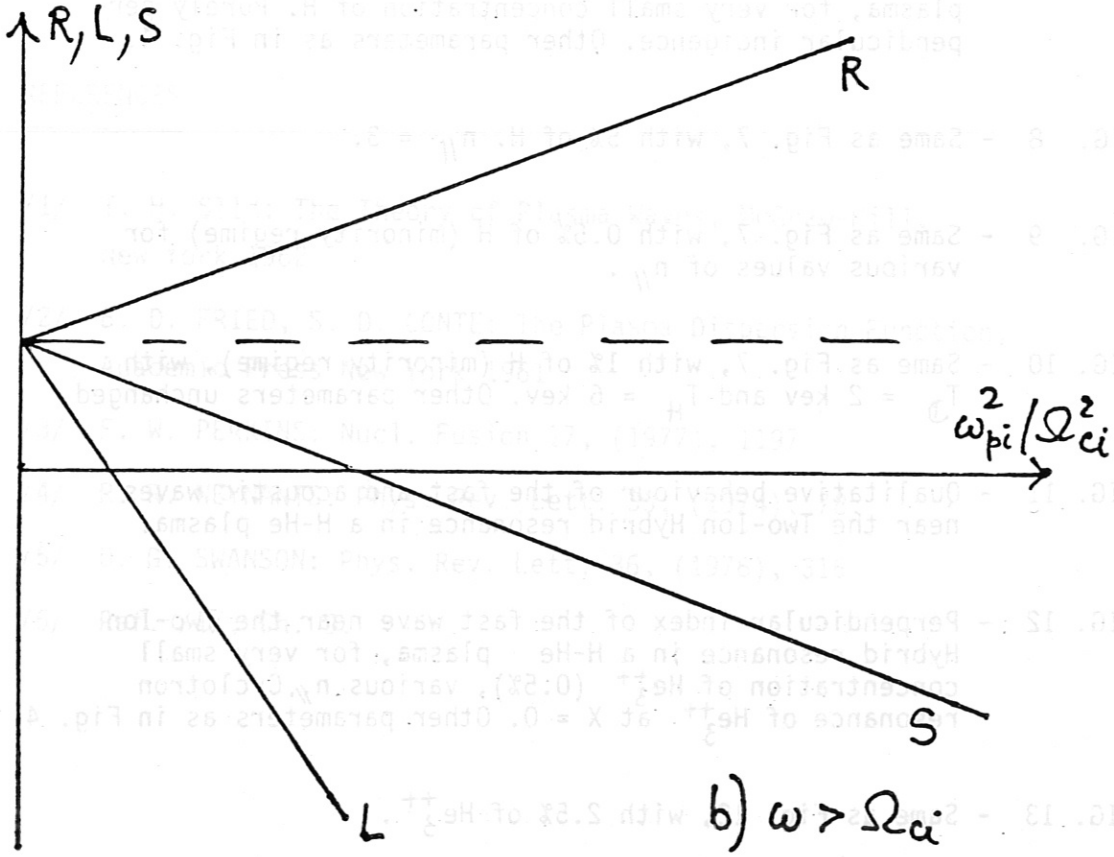
R,L,S
R
$\omega_{pi}^2/\Omega_{ci}^2$
S
L
b) $\omega > \Omega_{ci}$

FIG. 1

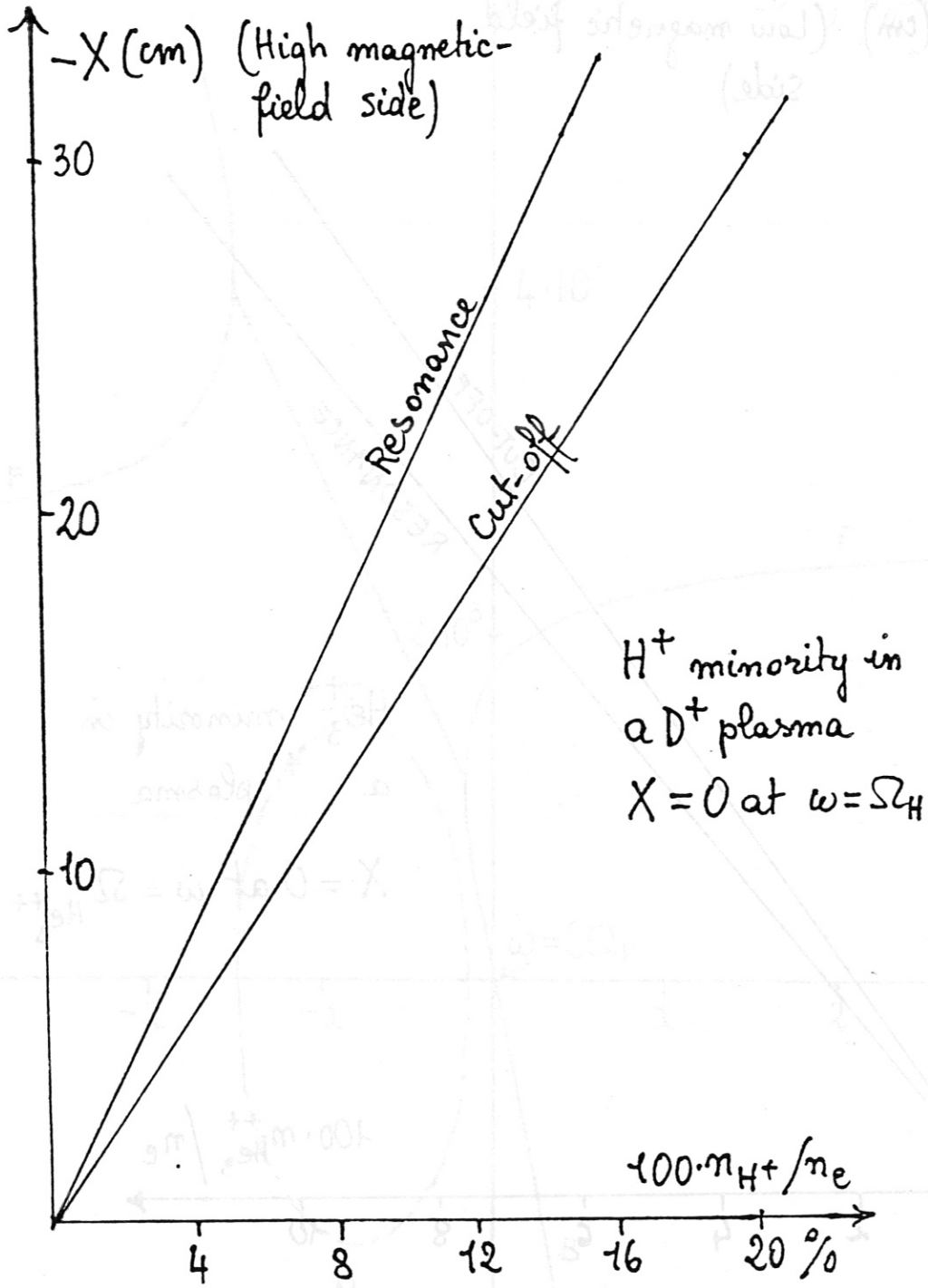
-X (cm) (High magnetic-field side)
30
20
10
Resonance
Cut-off
H+ minority in a D+ plasma
X = 0 at ω = Ω_H
100·n_H+/n_e
4
8
12
16
20 %

FIG. 2

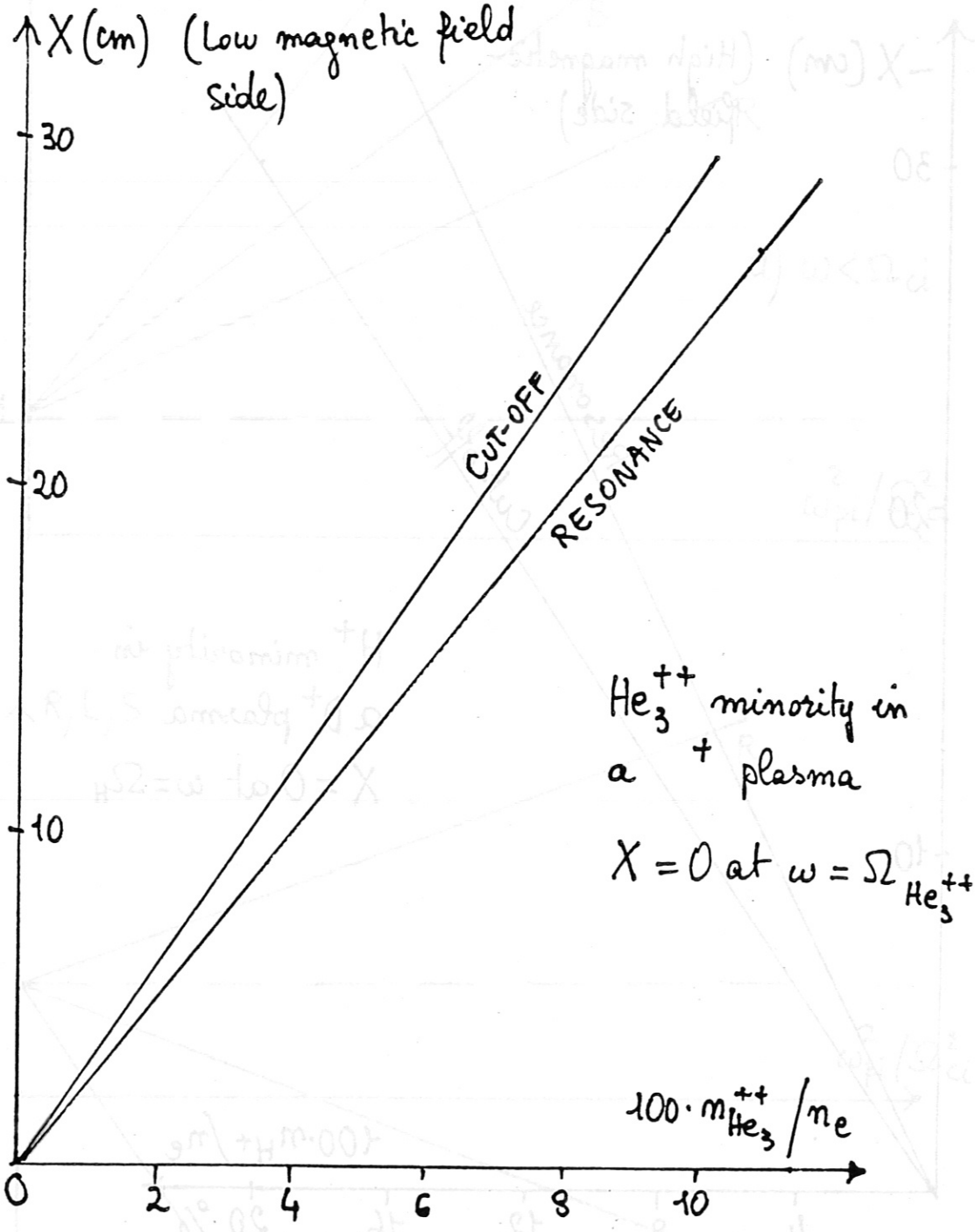
X (cm) (Low magnetic field side)
30
20
10
CUT-OFF
RESONANCE
He_3^{++} minority in a $^+$ plasma
$X = 0$ at $\omega = \Omega_{He_3^{++}}$
$100 \cdot m_{He_3}^{++} / n_e$
0
2
4
6
8
10

FIG. 3

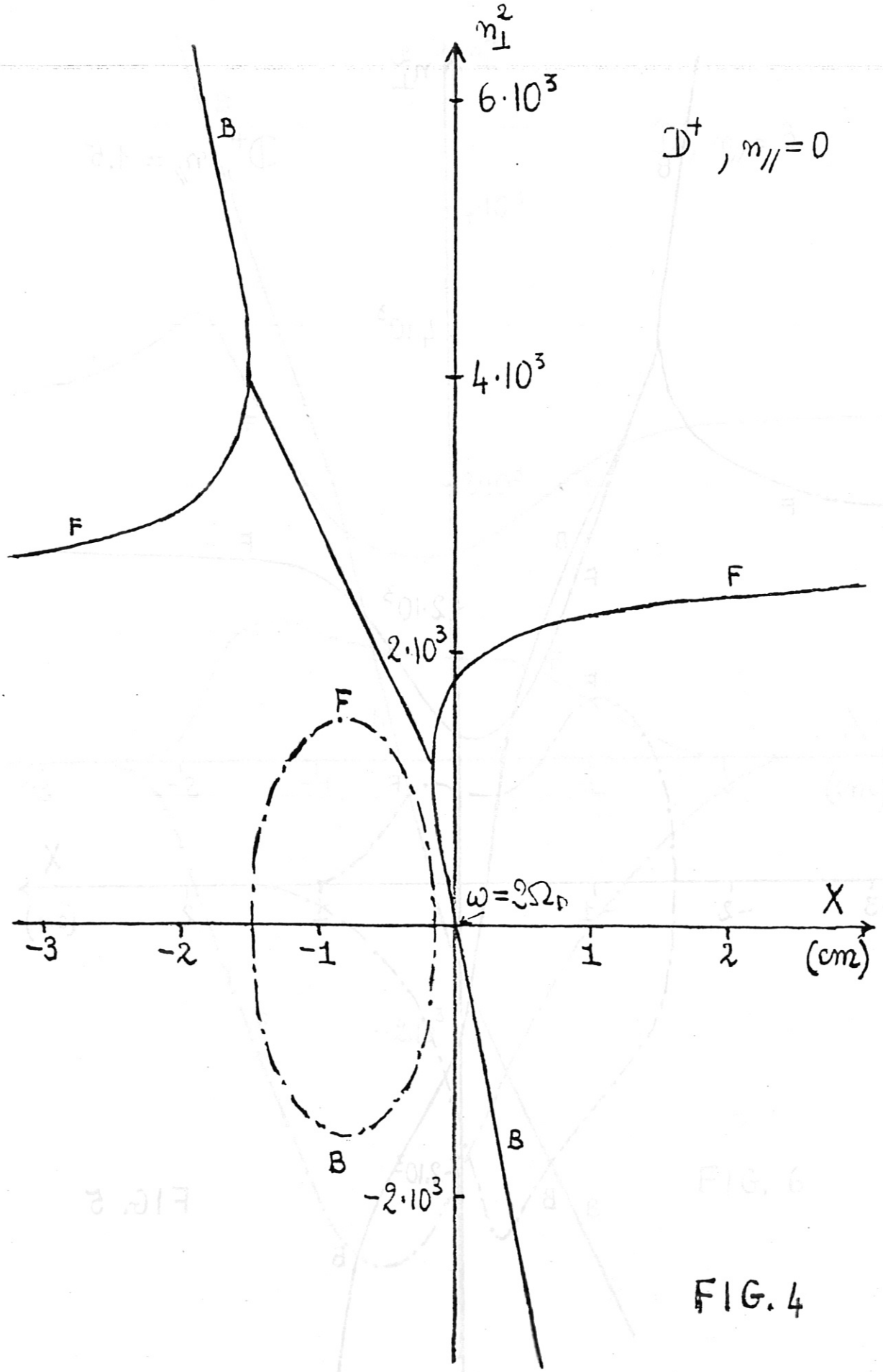
$n_\perp^2$
$6\cdot10^3$
$4\cdot10^3$
$2\cdot10^3$
$-2\cdot10^3$
D^+, $n_{//}=0$
B
F
F
F
B
B
$\omega=2\Omega_D$
X
-3
-2
-1
1
2
(cm)

FIG. 4

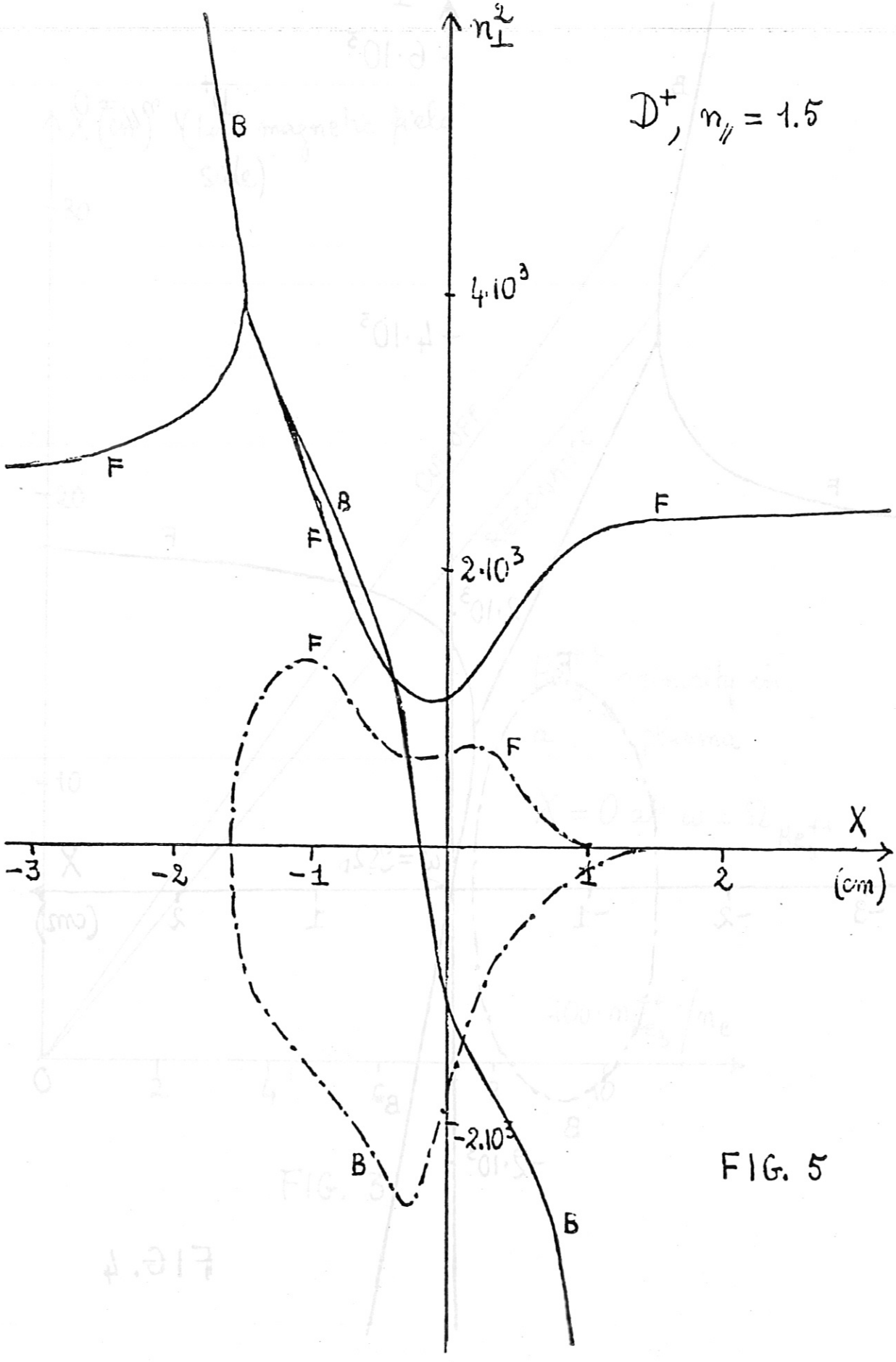
$n_\perp^2$
D^+, $n_{//} = 1.5$
B
F
B
F
F
$4 \cdot 10^3$
$2 \cdot 10^3$
F
F
F
X
-3
-2
-1
1
2
(cm)
B
$-2 \cdot 10^3$
Б

FIG. 5

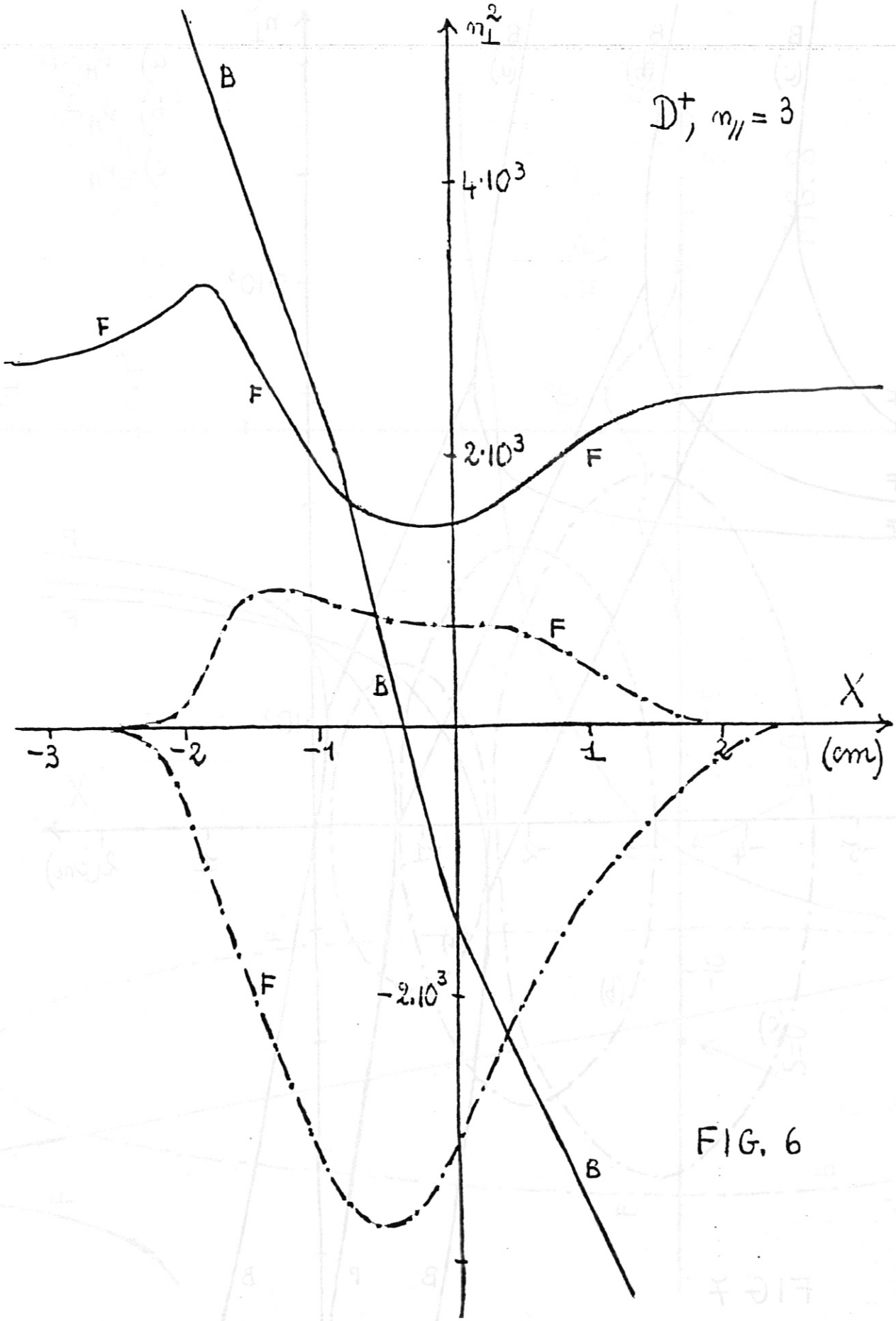

FIG. 6

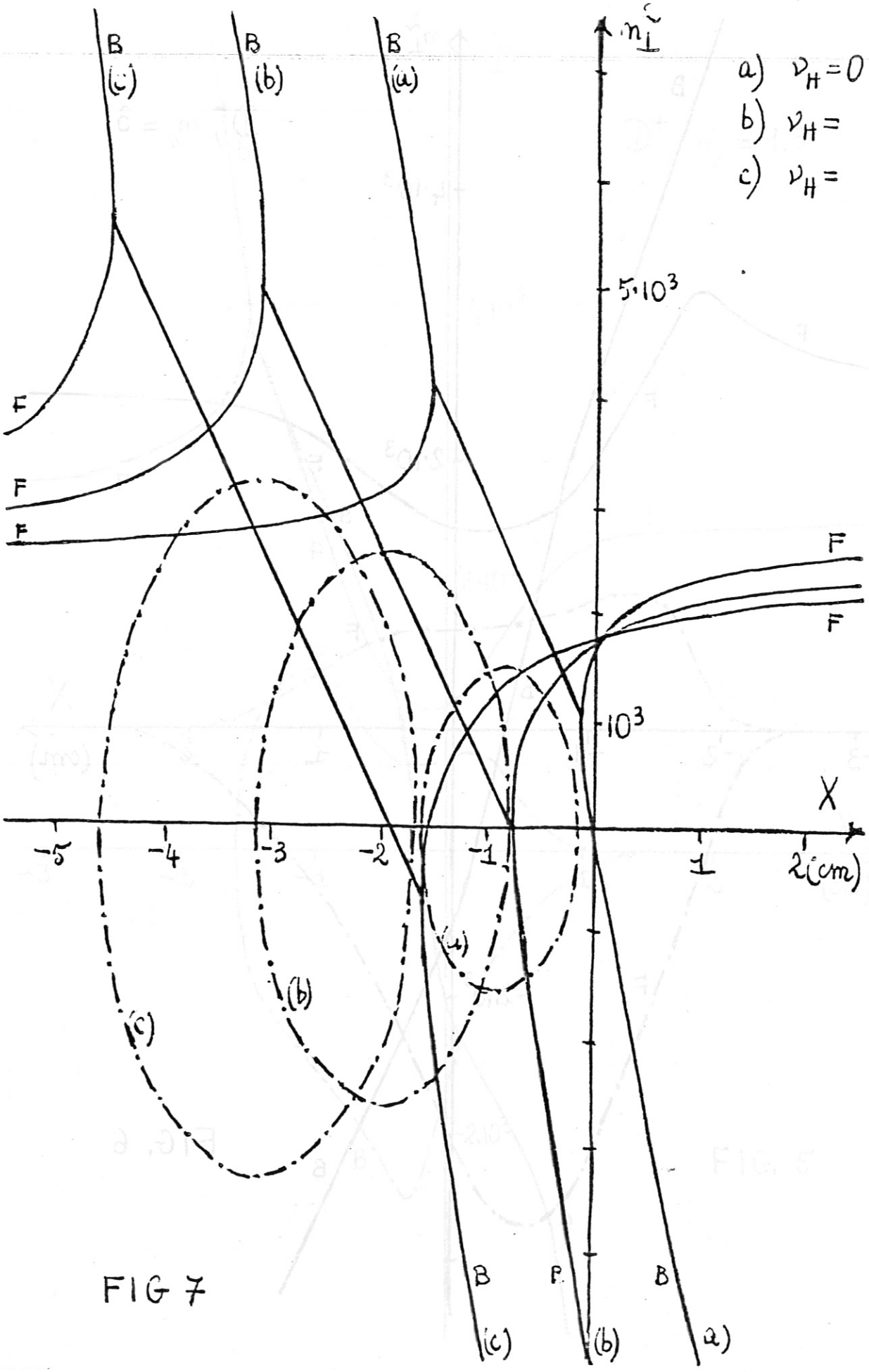
B
(c)
B
(b)
B
(a)
$n_\perp$
a) $\nu_H = 0$
b) $\nu_H =$
c) $\nu_H =$
$5 \cdot 10^3$
F
F
F
F
F
10^3
X
-5
-4
-3
-2
-1
1
2(cm)
(a)
(b)
(c)
B
F
B
(c)
(b)
a)

FIG 7

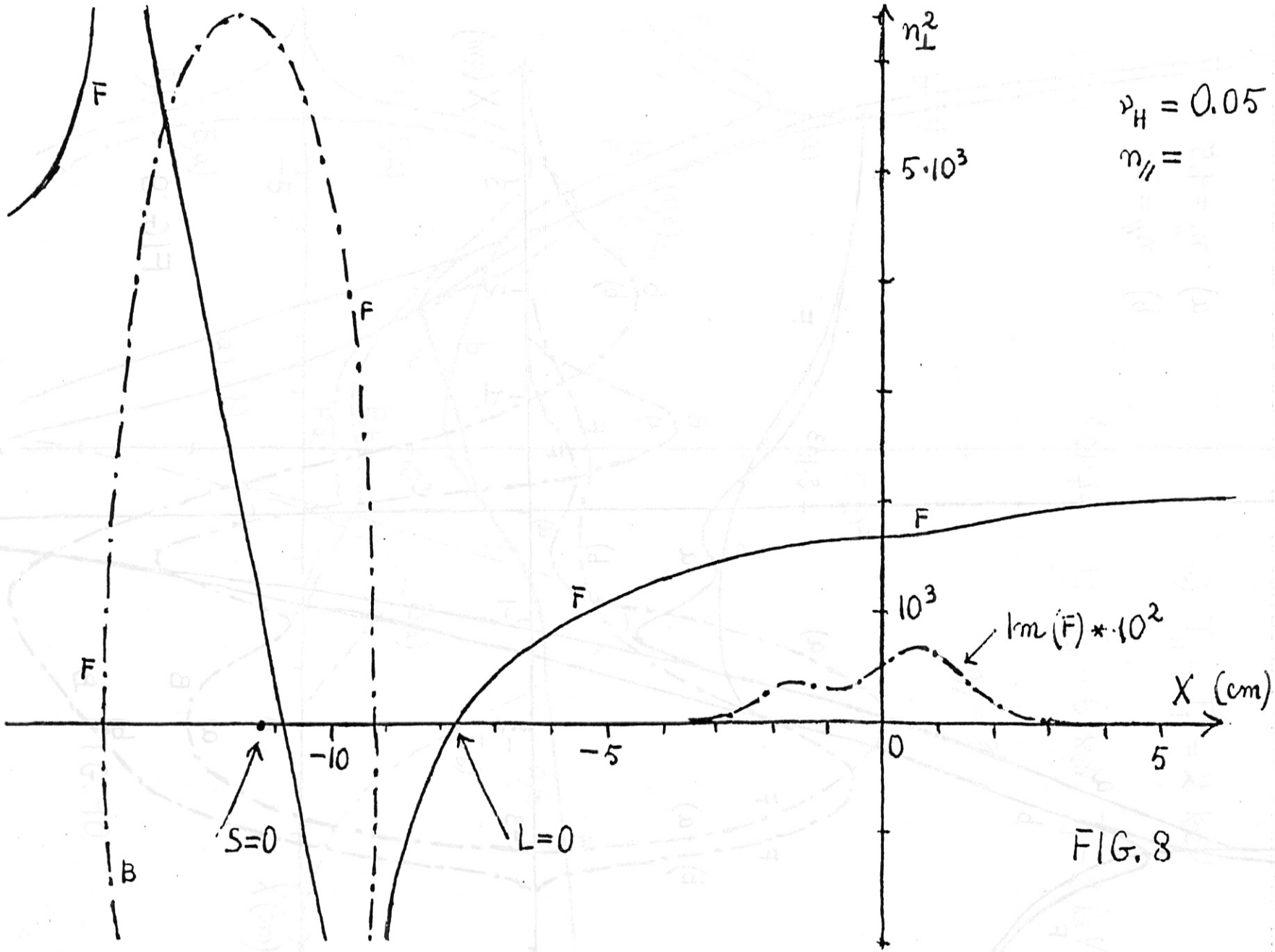

FIG. 8

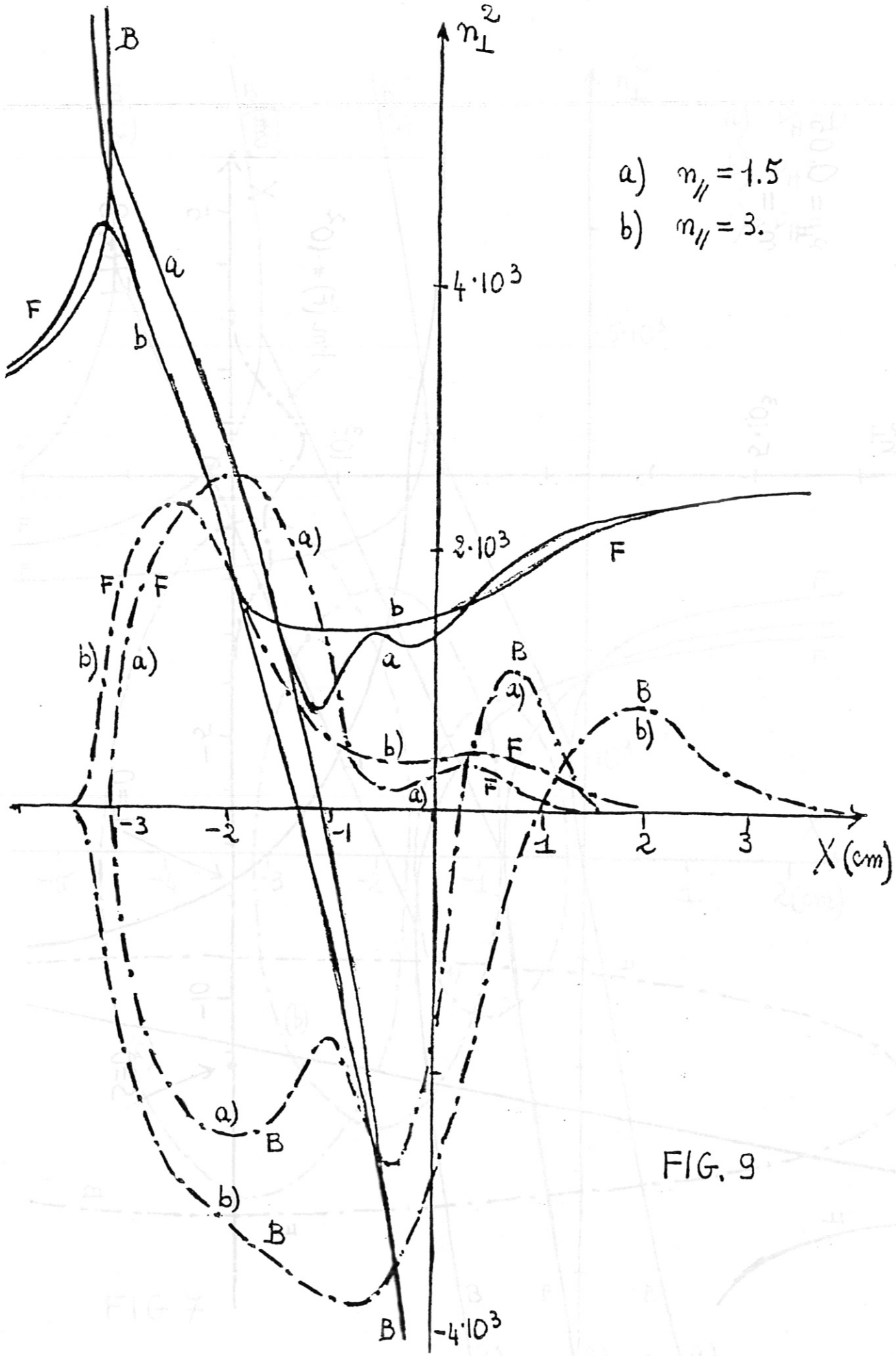
a) $n_{//} = 1.5$
b) $n_{//} = 3.$
$n_\perp^2$
$4 \cdot 10^3$
$2 \cdot 10^3$
$-4 \cdot 10^3$
B
F
a
b
-3
-2
-1
1
2
3
X (cm)

FIG. 9

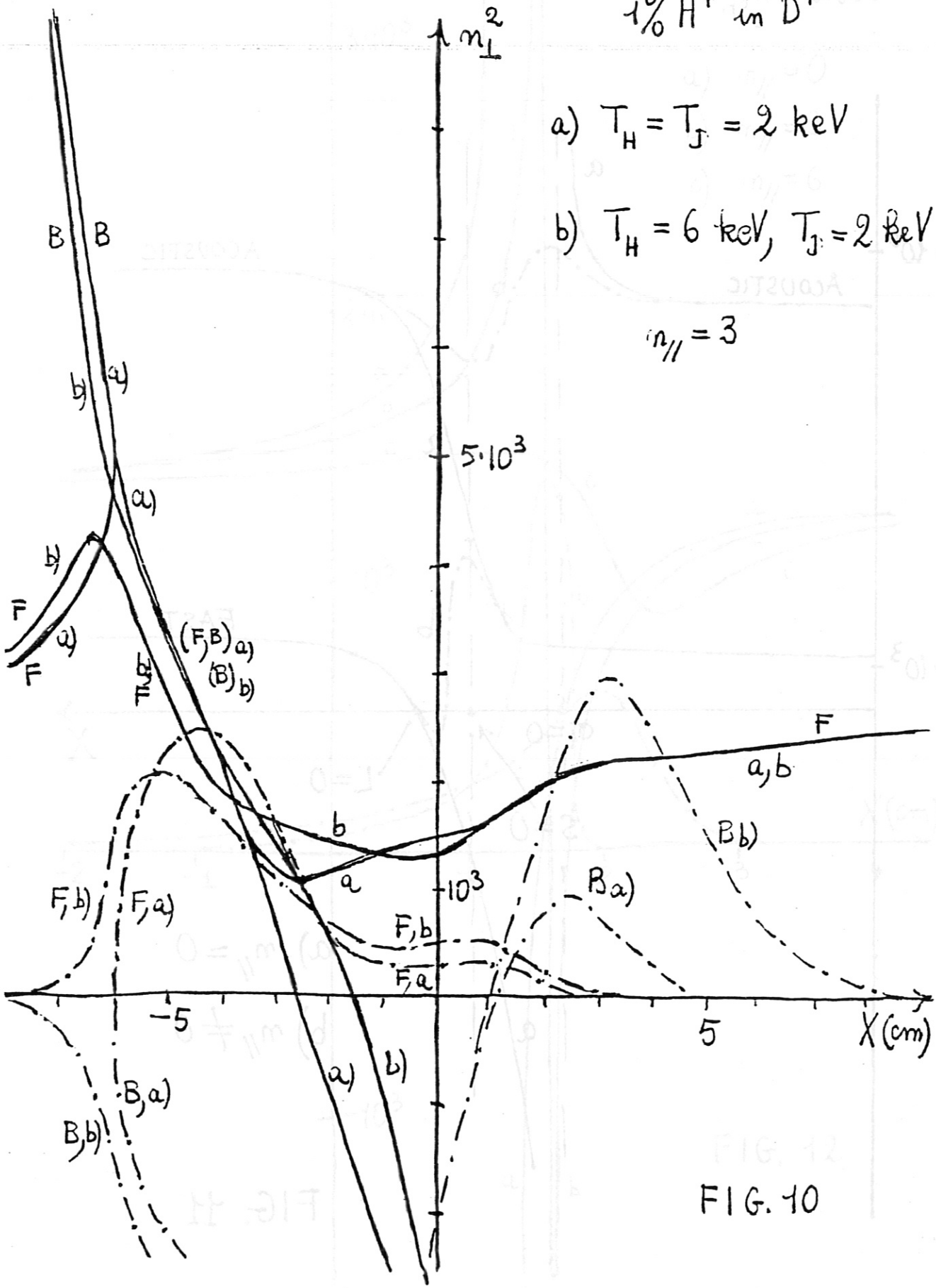
1% H+ in D+
a) T_H = T_J = 2 keV
b) T_H = 6 keV, T_J = 2 keV
n// = 3
n⊥²
5·10³
10³
B B
b) a)
a)
b)
F
a)
(F,B) a)
(B) b)
F
a,b
b
a
Bb)
Ba)
F,b)
F,a)
F,b
F,a
-5
5
X (cm)
a) b)
B,a)
B,b)

FIG. 10

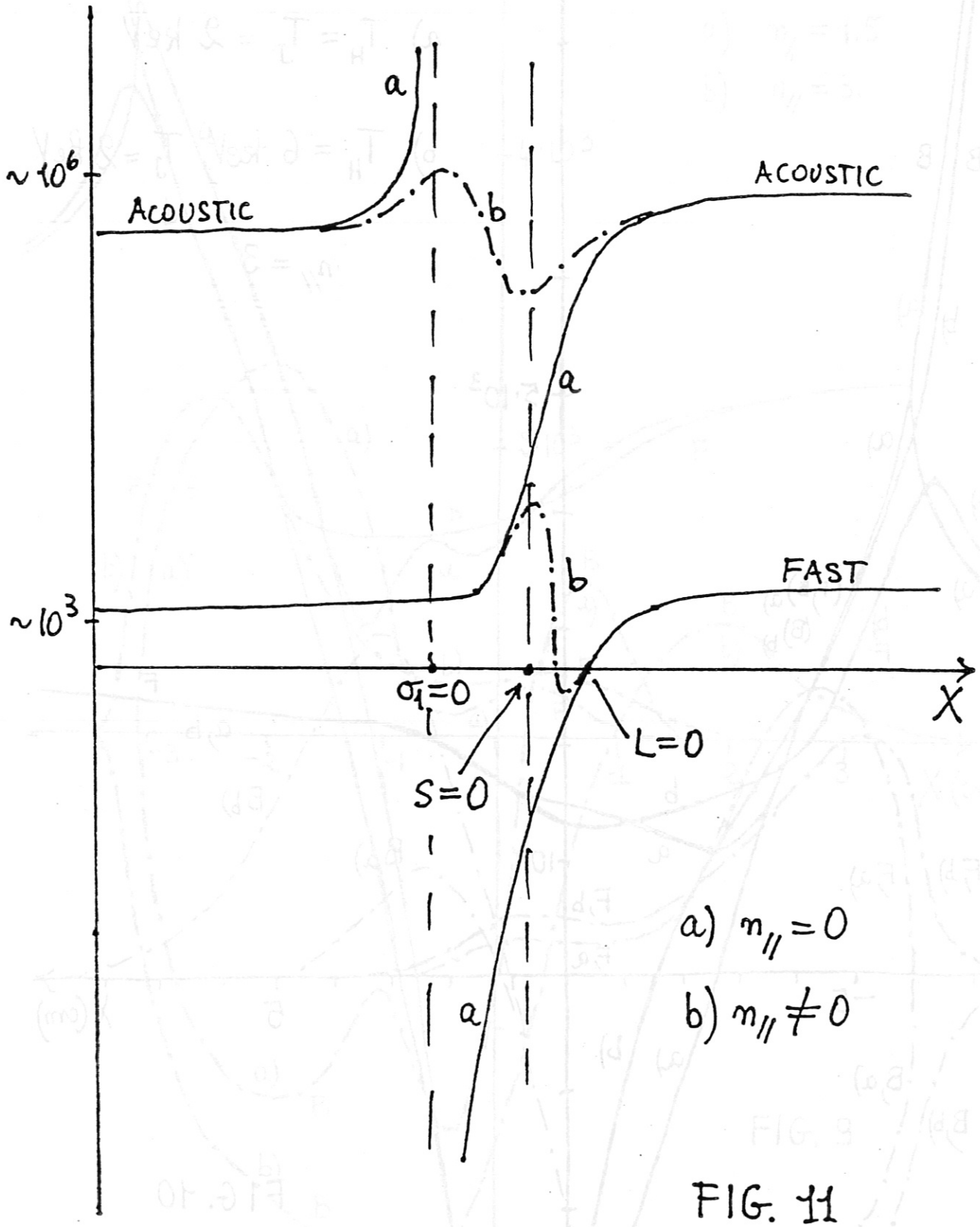

FIG. 11

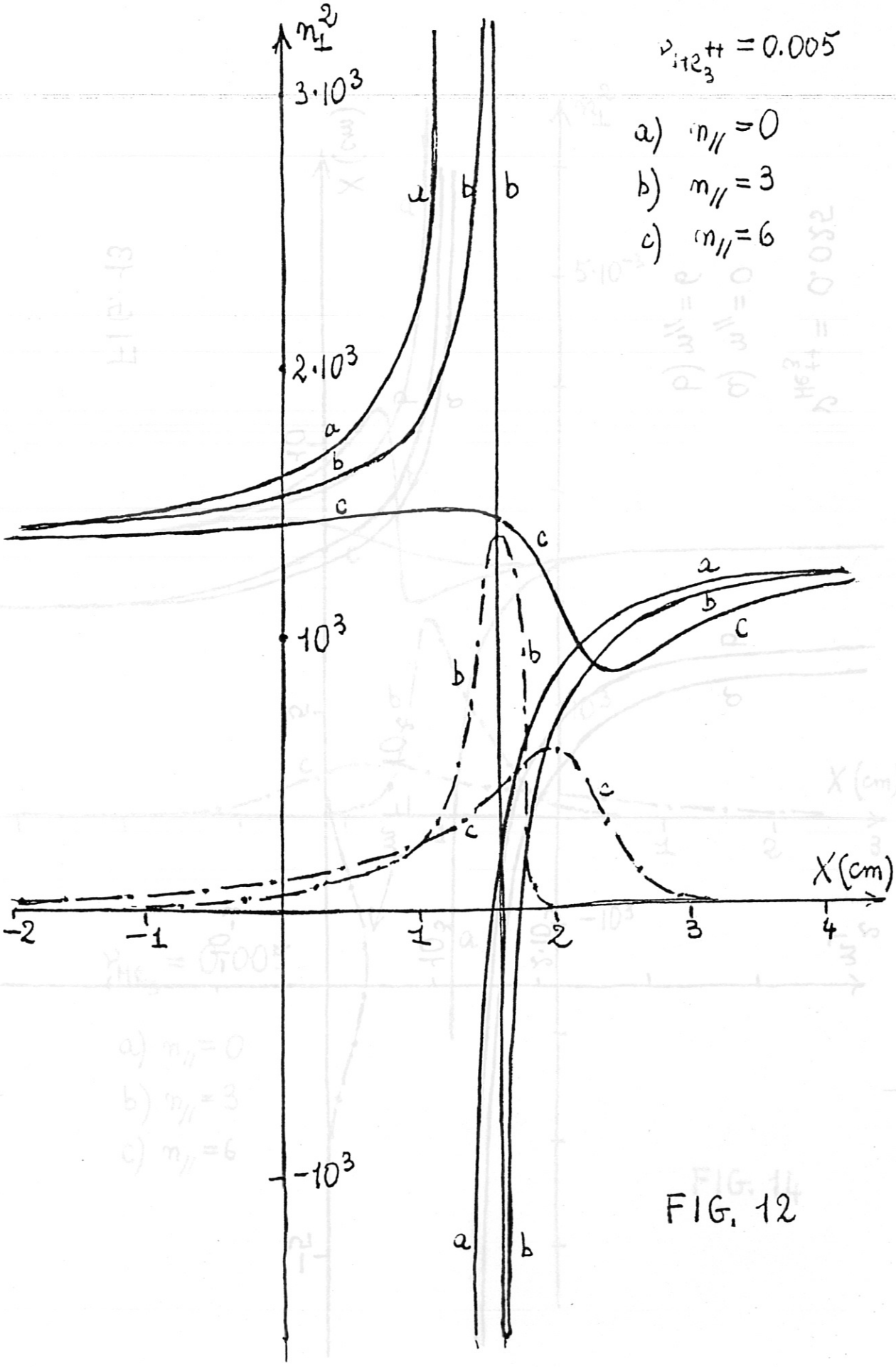
$n_\perp^2$
$3 \cdot 10^3$
$2 \cdot 10^3$
10^3
-10^3
$\nu_{i+12_3^{++}} = 0.005$
a) $n_{//} = 0$
b) $n_{//} = 3$
c) $n_{//} = 6$
X(cm)
-2
-1
1
2
3
4

FIG. 12

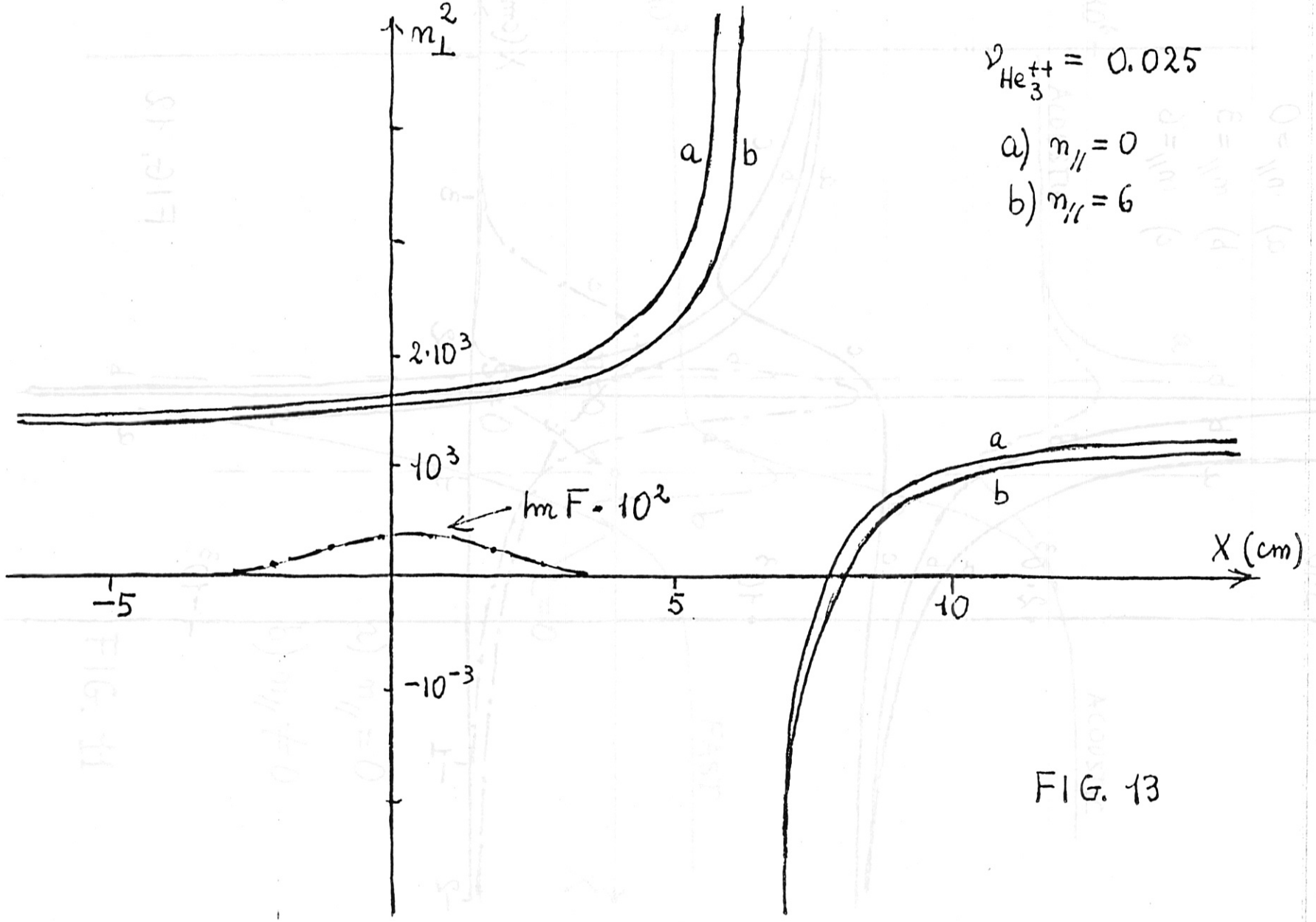
$n_\perp^2$
a
b
$2 \cdot 10^3$
10^3
$\mathrm{Im}\, F \cdot 10^2$
-10^{-3}
−5
5
10
X (cm)
$\nu_{He_3^{++}} = 0.025$
a) $n_{//} = 0$
b) $n_{//} = 6$

FIG. 13

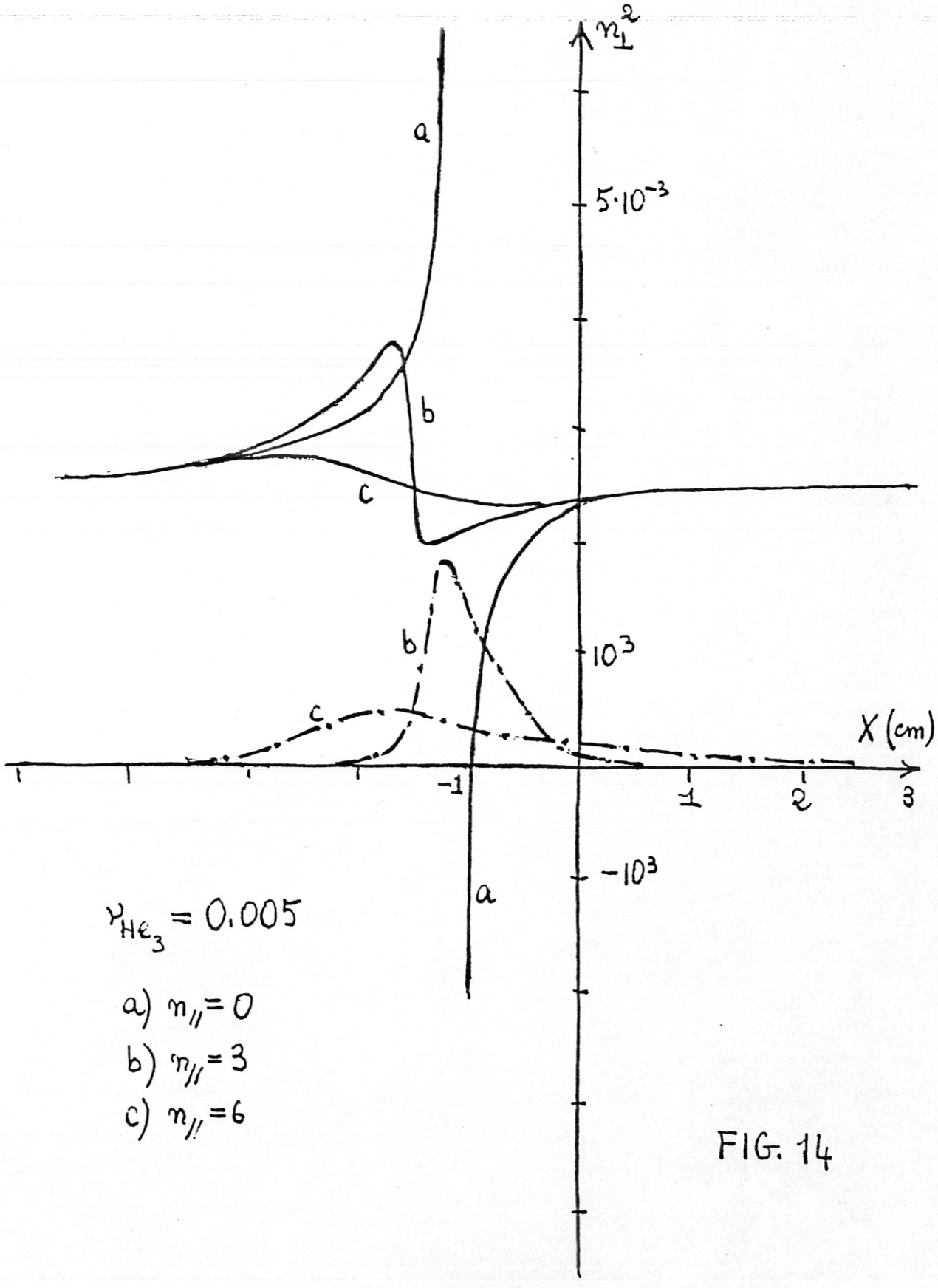

$\nu_{He_3} = 0.005$

a) $n_{//} = 0$

b) $n_{//} = 3$

c) $n_{//} = 6$

FIG. 14